Evaluating the influence of establishing pine forests and switchgrass fields on local and global climate

Benjamin J. Ahlswede

Dissertation submitted to the Faculty of the
Virginia Polytechnic Institute and State University
in partial fulfillment of the requirements for the degree of

Doctor of Philosophy
in
Forest Resources and Environmental Conservation

R. Quinn Thomas, Chair
Thomas L. O'Halloran
Randolph H. Wynne
John E. Barrett

April 9, 2021
Blacksburg, Virginia

Keywords: land cover change, bioenergy, albedo, carbon, radiative forcing, surface temperature, eddy covariance

Evaluating the influence of establishing pine forests and switchgrass fields on local and global climate

Benjamin J. Ahlswede

(ABSTRACT)

Humans have extensively altered terrestrial surfaces through land-use and land-cover change. This change has resulted in increased food, fiber, fuel, and wood that is provisioned by ecosystems to support the human population. Unfortunately, the change has also altered climate through carbon emissions and changes in the surface energy balance. Consequently, maximizing both the provisioning and climate regulation services provided by terrestrial ecosystems is a grand challenge facing a growing global population living in a changing climate. The planting of pine forests for timber and carbon storage and switchgrass fields for bioenergy are two land-cover types that can potentially be used for climate mitigation. Importantly, both are highly productive systems representing contrasts in albedo (grass are brighter than pines) and vegetation height (pines are taller than the grass) along with unknown differences in carbon and water balance that influence local to global climate. Here I use eddy-covariance data to investigate how a transition from a perennial bioenergy crop (switchgrass) to a planted pine plantation alters the local surface temperature, global carbon dioxide concentrations, and global energy balance. First, I found that switchgrass and pine ecosystems have very similar local surface temperatures, especially during the grass growing season. After the switchgrass is harvested, surface temperature in the pine forest is much lower than switchgrass because no vegetation is present to facilitate the evaporation of water. The surface temperature in a bare-ground system (a recent clear-cut) was also

high relative to the pine and pre-harvest switchgrass ecosystems. This illustrates the importance of maintaining vegetation cover to reduce local surface temperature. Second, I found that the 30-year mean change in global energy balance (i.e., radiative forcing) from planting a pine ecosystem rather than a switchgrass field was positive (pine warms climate) when considering changes in albedo and carbon measured using eddy-covariance systems. When including harvested carbon, pine and switchgrass can have similar global radiative forcing if all harvested pine carbon is stored, but harvested switchgrass carbon is burned. However, no scenarios I explored resulted in a strong negative radiative forcing by the pine ecosystem relative to the switchgrass field. These results show that afforestation or reforestation in the eastern United States may not result in any climate benefit over planting a switchgrass field. However, the presence of vegetation in both ecosystem types offers a clear benefit by cooling local surface temperatures.

Evaluating the influence of establishing pine forests and switchgrass fields on local and global climate

Benjamin J. Ahlswede

(GENERAL AUDIENCE ABSTRACT)

Humans are changing the Earth's climate by using oil and gas as fuel that emits greenhouse gases, mainly carbon dioxide, into the atmosphere. Planting trees to reestablish forests is a natural solution for climate change because forests absorb carbon dioxide from the air, but reforestation also changes the Earth's climate in other ways. For example, forests are generally darker than crops and grasses and absorb more sunlight, which traps energy in the atmosphere that can warm global temperature. These non-carbon effects can potentially offset the climate benefit from absorbed carbon dioxide. An alternative natural climate solution is to replace oil and gas with fuels derived from plants, known as bioenergy. Here I compared the local and global climate influence of a tree plantation (loblolly pine) to a bioenergy crop (switchgrass). I found that the local temperature of pine and switchgrass were similar in the summer when the grass was growing, and both were cooler than bare-ground, which was unable to evaporate and transpire water to the atmosphere. Over 30 years, I found that pine and switchgrass absorb similar amounts of carbon. The pine forest absorbs more carbon than switchgrass when it is fully grown but releases carbon during the first five years of growth. As a switchgrass field is brighter than a pine forest, planting a pine forest instead of a switchgrass field warms the Earth's climate. However, assuming no carbon from the harvested trees is released to the atmosphere, the pine and switchgrass have the same influence on global climate. My findings show that a pine plantation and a bioenergy crop can have similar climate benefits when carbon is stored in forests.

Dedication

For Lyana and Evelyn

If you simply refuse to quit, even the impossible can be accomplished.

Acknowledgments

No project of this magnitude is completed independently. I would like to acknowledge and thank the many people and institutions that have supported me and this project over the years. Funding for this project was provided from USDA-NIFA (Projects 2015-67003-23485 and 2017-68002-26612), Virginia Tech's Global Change Center, within the Fralin Life Sciences Institute, the Forest Resources and Environmental Conservation Department of Virginia Tech. Linda Fink, David Hawkins and Sweet Briar College provided the use of the land and logistical support. Joshua Rady, Wyatt McCurdy, Natalie Jones, and James LeMoine, Michael Kline, Laura Puckett, Michael Graham assisted with field work, data collection and site maintenance. Tom O'Halloran has been my eddy covariance guru and taught how to splice electrical cables together while dangling of a 40 meter tall tower. Quinn Thomas, my principal advisor for both my Masters and the PhD, taught me too many things to list, but has been a constant source of support. I don't know if I'll every be the scientist you are, but thank you for taking me under your wing and showing me the way. My family, Karl, Sandy, Greg and Elaine all provided substantial emotional and financial support, especially during the challenging final year. My children, Lyana and Evelyn, who both joined us during this phase of my life, provided lots of giggles and laughter and hugs and snuggles and kisses and reminded me that my actual job is to function as a human jungle gym. Finally, I need to acknowledge my wife and partner, Sarah Ahlswede, without whom this truly would not have happened. Neither of us envisioned the challenges we would face when I started this process, but you took them all in stride. My name is on the document, and I'll have the PhD listed after my name, but this accomplishment belongs to you just as much as me. Congratulations Sarah, very well done.

Contents

List of Figures

List of Tables

Chapter 1

Introduction

Humans have extensively altered the land surface through land-use and land-cover change (Hurtt et al., 2006). This change has resulted in an increase in food, fiber, fuel, and wood provisioned by ecosystems to support the human population. Unfortunately, the change has also altered climate through carbon emissions and changes to the surface energy balance (Bonan, 1997, Pongratz et al., 2011). Approximately 10% of carbon emissions that drive climate change are from deforestation that converts forest to fields for crops and livestock (Cavallaro et al., 2018, Friedlingstein et al., 2020). Global ecosystems are also valued, at least implicitly, for their capacity to regulate climate (Bastin et al., 2019, Costanza et al., 2014, Pacala, 2004). For example, terrestrial ecosystems across the globe absorb $\sim$ 30% of the annual emissions, thus reducing the impact of current emissions on climate (Friedlingstein et al., 2020). Consequently, maximizing both the provisioning and climate regulation services provided by terrestrial ecosystems is a grand challenge facing a growing global population living in a changing climate.

Land-cover in temperate latitudes can be highly heterogeneous, with forests, pastures, and croplands co-existing on the landscape (Hansen et al., 2013). As a result, conversions among ecosystems that differ strongly in carbon, energy, and water cycling are common. This is particularly the case in the southeastern United States (SEUS), where short-rotation plantation forestry can trade-off with agricultural uses, including perennial biofuel crops (Wear and Greis, 2012). As the utilization of ecosystems for climate mitigation is increasingly considered in decisions (Hemes et al., 2021), quantifying how contrasting ecosystem types, such as tall pine plantation forests vs. short croplands, influence climate is necessary to evaluate trade-offs in mitigation capacity among ecosystems. Furthermore, understanding the mechanisms that drive the influence of terrestrial ecosystems on climate can help inform particular decisions, like which plant species to establish or the timing of management activity, that could aid in maximizing climate mitigation capacity.

While it is well established that land-cover change has an impact on climate by influencing the global carbon balance through losses from respiration and fire and gains from carbon storage in biomass, it is also critical to consider the biogeophysical climate forcing from land-cover change. Forests are darker than crops and grasses, and their tall canopies can cover snow, thus decreasing albedo at the surface (Betts, 2000, Bonan, 2008b, Jackson et al., 2008). Albedo, the ratio of outgoing to incoming solar radiation, alters climate by reflecting shortwave solar radiation back to space and reducing the total energy contained within the Earth system. Land-cover change can also alter evapotranspiration (ET), which is the total water vapor transpired and evaporated at the surface. ET cools the surface where the water is vaporized, but the energy contained in the water vapor is released upon condensation higher in the atmosphere. Furthermore, a change in ET, and thus atmospheric water content, will affect how clouds form in the atmosphere. Clouds increase planetary albedo and also increase the insulation of long-wave radiation emitted from the Earth's surface (Bonan, 2008a). Therefore, the exact effect from a change in cloudiness is complex, but these indirect climate effects can significantly impact global climate (Bala et al., 2007). Some ecosystem types, such as forests, have been shown to maintain higher ET than others, such as herbaceous grasslands, due to deeper rooting depth (Bonan, 2008a). In addition, other less well established biogeophysical forcings include changes to aerosol production (Unger, 2014).

Evaluating the combined influence of ecosystem biogeochemical (i.e., carbon cycle) and biogeophysical processes on climate is challenging. Importantly, biogeophysical and biogeochemical processes influence climate at different spatial scales. The ecosystem carbon balance influences atmospheric CO_2 concentrations, which are well-mixed throughout the atmosphere, resulting in a global influence of local land-cover change. Changes in albedo alter the radiative balance at the top of the atmosphere, which, similar to carbon, can

have a regional to global influence on climate. However, changes in albedo also have local influences by trapping more or less energy at the vegetation surface. This energy heats surface temperatures and powers the transfer of energy to the near-surface (i.e., local) atmosphere via latent or sensible heat. Furthermore, the energy transfer efficiency can be governed by the ecosystem's height. As a result, changes in the carbon, energy, and water cycles have local to global influences on climate that should be quantified and compared when evaluating an ecosystem's climate mitigation potential. This is especially important when climate mitigation is an explicit objective for converting among ecosystems, as is the case when bioenergy crops are established or forests are planted for carbon credits.

Eddy covariance (EC) flux towers are among the best tools available for quantifying the biogeochemical and biophysical influences of ecosystems on climate (Hemes et al., 2021). They measure the net movement of heat, carbon dioxide, water, and other trace gases, into and out of the land-surface they are situated over (Aubinet et al., 2012, Baldocchi et al., 1988). Unlike global climate models and many satellite products, the scale of measurements from an EC study is limited to a small homogeneous area representing the ecosystem of interest. Furthermore, flux towers often include meteorological measurements of radiation and temperature that are necessary for determining surface temperatures. When multiple flux towers are located close to each other, but over different land types, they are an ideal tool for studying the effect that LCC has on climate because they are standardized for soil and local meteorology (Baldocchi, 2014). Overall, flux observations directly measure differences in local climate, and their observations can be linked with simple models of global energy balance to evaluate the global scale influences Kirschbaum et al. (2011).

My dissertation focuses on evaluating the local to global influence of land-cover change using flux towers, including a set of co-located flux towers that were established as part of this project. In particular, I compare how the establishment of two contrasting

ecosystem types used for climate mitigation influence carbon, energy, and water balances: perennial bioenergy grasses and pine plantation ecosystems. Both are highly productive systems representing contrasts in albedo (grasses are brighter than pines) and vegetation height (pines are taller than grasses) along with unknown differences in carbon and water balance. Within the southeastern United States (SEUS), both ecosystems are actively used on the landscape for production. The region is one of the world's largest producers of wood products, and the majority of these wood products come from planted southern yellow pine (Wear and Greis, 2013). The specific species of this variety are longleaf pine (*Pinus palustrus*), shortleaf pine (*Pinus echinata*), slash pine(*Pinus elliottii*), and loblolly pine(*Pinus taeda*). Planted southern pine trees grow quickly and are typically harvested after 20-30 years. Common uses of southern pine wood include paper production and timber products. However, there is increased interest in the use of pine biomass as a source of bioenergy (Wear and Greis, 2013). The SEUS region also includes historical and current sources of non-woody bioenergy species, such as corn ((*Zia mays*), sugarcane (*Saccharum officinarum*), *Miscanthus*, and switchgrass (*Panicum virgatum*) (Yadav et al., 2019). Switchgrass has emerged as an ideal bioenergy crop due to its fast growth, high yields, deep roots, and minimal management requirements (Parrish and Fike, 2005, Wright, 2007). Furthermore, switchgrass has higher albedo than traditional row crops (Miller et al., 2016) and forests (Jackson et al., 2008), improving the argument for switchgrass bioenergy as a climate change mitigation strategy. Switchgrass and southern pine share a large common range, and in some cases, can be planted together (Albaugh et al., 2014). Pine and switchgrass are not typically thought of as competitors for land allocation. However, since both are candidates for bioenergy production, and an increase in demand for bioenergy would require the expansion of their ranges, the climate forcing of converting from one land type to the other needs to be assessed.

Using flux towers, I quantify the carbon, energy, and water differences between switchgrass fields and pine plantations and use these observations to model the differences in local surface temperatures and global radiative forcing. First, in Chapter 2, I evaluate the surface temperature differences among the set of new co-located flux towers located in the piedmont of Virginia. These towers include a 30-year-old loblolly pine plantation, a 5-year-old switchgrass field, and a recent loblolly pine clearcut. This chapter uses the contrasts in vegetation (vegetated grass and pine vs. bare soil clearcut) and height (top pine vs. short grass and clearcut) to isolate mechanisms that drive the observed changes in surface temperature. Second, I quantify the differences in carbon storage between the pine and switchgrass ecosystems at the co-located flux towers. Chapter 3 specifically focuses on the switchgrass field's carbon balance since no prior studies have reported on eddy-covariance measurements from switchgrass in a similarly warm and wet climate. Finally, in Chapter 4, I evaluate the global radiative forcing resulting from a conversion from switchgrass to pine. This chapter includes a new synthesis of carbon storage and albedo observations from pine plantations and switchgrass eddy-covariance studies across eastern North America to model the drivers of radiative forcing over full harvest rotations. Overall, my dissertation clearly demonstrates the complexities of relying on terrestrial ecosystems for climate mitigation: vegetated ecosystems reduce local surface temperatures but can increase global radiative forcing.

Chapter 2

Presence of vegetation is the dominant driver of land-cover change induced surface temperature differences

2.1 Abstract

Evaluating the influence of land-use and land-cover change (LULCC) on land-surface temperature (T_s) is critical for effectively using land management as a climate mitigation solution. Quantifying this influence in the temperate zone is of particular interest due to the diverse land-use and land-cover across the region and uncertainty in direction, magnitude, and mechanism of T_s changes. Here we examine how three co-located ecosystems representing contrasts in vegetation presence and height (pine plantation, switchgrass field, and a bare-ground clearcut in Virginia, USA) influence T_s. We found that during the growing season, the clearcut was $>3°C$ warmer than both grass and pine systems, but the difference between grass and pine was small ($0.3°C$). During the dormant season, the grass T_s increased relative to the pine stand and was nearly identical to the clearcut. The primary mechanism for the cooling effect of two vegetated systems in early summer was latent heat flux. Our study highlights that ecosystem management for surface climate mitigation in the temperate region may benefit from first focusing on the presence of vegetation throughout the year rather than on the use of a specific vegetation type.

2.2 Introduction

Land-use and land cover change, specifically deforestation and reforestation, alter the energy balance and temperature (T_s) of the land surface (Jackson et al., 2008). Managing land for the biophysical influence on local to global temperatures has been proposed as a component of climate change mitigation (Hemes et al., 2021). However, the influence that land cover change can have on T_s depends on the latitude where the change occurs, thus adding complexity to the use of land-cover change as a mitigation tool (Bonan, 2008a, Lee et al., 2011). For example, deforestation in boreal regions reduces T_s by reducing net radiation through an increase in albedo (Betts, 2000). In contrast, deforestation in tropical regions, where albedo differences between forested and deforested systems are minor (due to a lack of snow), deforestation increases T_s due to decreased evapotranspiration (Bonan, 2008a). In temperate regions, changes to T_s from deforestation have been uncertain. However, recent observational evidence suggests conversion of forests to grasses or crops would increase average T_s (Burakowski et al., 2017, Chen et al., 2019, Lee et al., 2011, Li et al., 2015, Zhang et al., 2020). Studies to date have focused on the influence that deforestation and afforestation have on T_s using a space for time substitution by comparing a forested ecosystem to a nearby short stature ecosystem, usually a grass species. However, the roles of the dynamics of the grass system have largely been ignored. Furthermore, the replacement a forest with a grassland assumes a reduction of the ability to absorb carbon dioxide(CO_2) (Pongratz et al., 2011). To date, no comparisons have been made between a forest and a highly productive grassland (i.e., bioenergy crop) regarding a change in T_s.

While forest and grass land-cover types are the beginning and ending point in a land-cover change that converts forest to agricultural or pasture land-uses, few studies include the intermediary stage where bare-ground is exposed following a clearcut of the forest. The bare ground state during land-cover change is critical in regions that experience frequent

disturbance through harvesting, such as short-rotation pine plantations in the southeastern United States (Hansen et al., 2013). This intermediary stage is non-vegetated, and its inclusion in the land-cover change studies allows more mechanistic investigation into the drivers of surface temperature change. In particular, including the bare-ground systems separates the influence of vegetation change (trees to grass) from the change in structure (tall to short stature ecosystems) that occurs following land-cover conversion from forest to grassland.

Here we examined the temperature and energy fluxes at three newly established co-located flux towers in a managed pine forest, a switchgrass field, and a bare-soil system that followed a clearcut. The towers are located in a humid subtropical climate (central Virginia, USA). We used the ecosystems contrasting structure to explore mechanisms of surface temperature change across the three towers. Specifically, we examined how surface temperature differs among the switchgrass, clearcut, and pine ecosystems during the growing and dormant seasons. Then, we quantified differences in the radiative and non-radiative energy budget of the three ecosystems combining bio-meteorology and eddy-covariance measurements to examine the temperature change mechanisms.

2.3 Methods

2.3.1 Site Description

Our study uses concurrent data from three co-located eddy covariance towers located in central Virginia. This regions climate is humid subtropical (Köppen climate classification Cfa), with warm humid summers and cool mild winters. The first tower (Ameriflux designation: US-SB1, Pine hereafter) is over a mixed-age loblolly pine (*Pinus taeda*) plantation.

The second tower (US-SB2, Grass hereafter) is over a switchgrass (*Panicum virgatum*) field harvested annually for bioenergy. The third tower (US-SB3, Clearcut hereafter) is over a recently harvested loblolly Pine stand (harvesting with removal in January 2018). These three towers are within 1.6 km of each other, ensuring that each system shares weather conditions and soil characteristics and allowing inference that observed differences are due to the differences in vegetation land cover.

The three towers were established at different times, with the Clearcut tower the most recent. The period with data available at all three towers started in March 2018. Therefore, we focused our analysis on 2018, when the Clearcut site was not vegetated; after 2018, early successional species began to establish at the Clearcut, and loblolly saplings were planted. Furthermore, the Pine tower suffered a significant lightning strike in the late summer of 2018, damaging some instruments and leading to data losses. Therefore, we further focus our analysis on the periods of time when data coverage of all three towers is sufficient. These periods are the early growing season from May 2 to July 5, 2018 (referred to here as "Early Summer"), and October 10 to December 8, 2018 (referred to here as "Autumn") (Figure: 2.4). These two periods of time cover two important phases of the switchgrass life-cycle: early summer covering the peak growing season, and autumn beginning immediately after the switchgrass was harvested. For analysis, we also divided our data into daytime and nighttime. To define nighttime conditions, we produced an aggregate S_i product from the S_i data streams of all three towers, and define daytime as $S_i >= 10\ w/m^2$ and night time as $S_i < 10\ w/m^2$.

2.3.2 Bio-meteorology Instruments

Each tower was equipped with a CNR4 four way net radiometer to measure the incoming and outgoing shortwave and long-wave radiation. Surface temperature (T_s) was inferred from the outgoing long-wave radiation (L_o) such that

$$T_s = \sqrt[4]{\frac{L_o}{\epsilon * \sigma}} \tag{2.1}$$

where σ is the Stefan-Boltzmann constant, and ϵ is the emissivity. Emissivity, in this case, was set to 0.95 for all three ecosystems. We based this emissivity value on the Ecostress satellite emissivity for these sites (Hook and Hulley, 2019). We chose the Ecostress emissivity product because it has high spatial and temporal resolution and is temporally overlapping data with our observations. Ecostress emissivity of the three land-cover types had considerable overlap and no relationship with time. Therefore, the average emissivity reported across sites was used (0.95). Albedo (α) was calculated daily from the ratio of mid-day (1100 - 1300) incoming (S_i) and outgoing (S_o) short-wave radiation ($\alpha = S_o/S_i$).

The CNR4 of the Pine tower was 26 meters above ground level, 4 - 6 meters above the upper canopy (20 - 22 meters in height). At the Clearcut and Grass towers, instruments were mounted on a tripod tower, with the CNR4 at a height of 4 meters and extended away from the tower base to avoid non vegetation in the instrument's view shed. The air temperature was measured at two heights on the Clearcut and Grass towers (2m and 4m) and at three locations on the Pine tower (2m, 26m, 34m) using an aspirated and shielded thermistor (HUMICAP HMP155) housed in a custom aspirated radiation shield. The air temperatures presented here are the uppermost air temperatures from each tower. Soil heat flux (G) was measured using Hukseflux HFP-01 soil heat flux plates buried 10cm below the ground surface.

2.3.3 Eddy Covariance Instruments and Products

Each tower was equipped with an eddy covariance (EC) system that was used to estimate the latent and sensible heat fluxes. Each EC system measured the temperature, water, and CO_2 concentrations of the atmosphere along with high frequency, three-dimensional wind direction, and wind speed measurements. Gas concentrations were measured with a closed-path infrared gas analyzer (LI-7200, Licor) at the Pine and Grass towers at 26 and 4 meters, respectively. The Clearcut tower was equipped with an open-path infrared gas analyzer at 4 meters (LI-7500, Licor). The Pine and Grass tower had a WindMaster Pro 3D sonic anemometer (Gill Instruments), and the Clearcut tower was equipped with a WindMaster 3D sonic anemometer (Gill Instruments). Data were collected continuously at 10 Hz and averaged to 30 minute time intervals using EddyPro version 6.2.2 (LI-COR, Inc., 2019).

To calculate latent and sensible heat fluxes, we implemented a double-rotation method to account for tilt in the anemometer, a block average detrending method, and compensation for density fluctuations. Quality checks were performed according to (Foken et al., 2004). Raw data were screened for spikes, amplitude resolution, drop-outs, absolute limits, skewness, and kurtosis according to Vickers and Mahrt (1997). Footprint estimation was performed according to (Kljun et al., 2004). Because this footprint model depends on canopy height, we supplied a dynamic height file to the EddyPro software that describes the switchgrass's changing height. Height was determined by visually inspecting PhenoCam images (Seyednasrollah et al., 2019), using a vertical PVC pipe in the field, marked every 10cm from the ground up to two meters. We did not include an angle of attack correction, as the available correction includes artificial inflation of the vertical wind measurement (LI-COR, Inc., 2019). The anemometer at the Pine tower is subject to the w-boost issue, and corrections were applied to offset the bias according to LICOR recommendations (Billesbach et al., 2019).

To remove data with inadequate turbulence, we applied a friction velocity (u*) filtering routine. This method removes observations where u*falls below a calculated threshold, indicating that fluxes cannot be calculated using the eddy covariance method. We determined the u*threshold by examining the relationship between u*and net ecosystem exchange fluxes as in Papale et al. (2006) using the REddyProc R-package (version 1.2) (Wutzler et al., 2018).

2.3.4 Analysis

Analysis was conducted based on half-hourly measurements of the variables described above. We first compare the average daily surface temperatures during the early summer and autumn time periods. We then analyzed the daytime and nighttime temperatures separately for each tower. We examined the mean diurnal course of air and surface temperatures by averaging each half-hour's value within a season. To examine energy flux differences we compared the average values for energy budget component during the early summer and autumn separately. We then use these energy budget calculations to examine the mechanisms by which land-cover change can affect T_s, albedo, Bowen ratio, and through changes in surface resistance (as measured by friction velocity (u*)).

2.4 Results

2.4.1 Surface Temperature

The average daily surface temperature was highest at Clearcut, while average surface temperatures were nearly identical between the Pine and Grass ecosystems. T_s at the Clearcut site was was 2.7 °C warmer than Grass and Pine (Figure: 2.1). During the daytime these

differences were larger, with the Clearcut site T_s 6.0 °C warmer than the Pine site and 4.5 °C warmer than the switchgrass site. During the day, the Grass site was slightly warmer (1.5 °C) than the Pine site. Average nighttime temperatures were similar between the three sites (< 1.5 °C). At night the Pine site was 1.4 °C warmer than the Grass site, and 0.9 °C warmer than Clearcut.

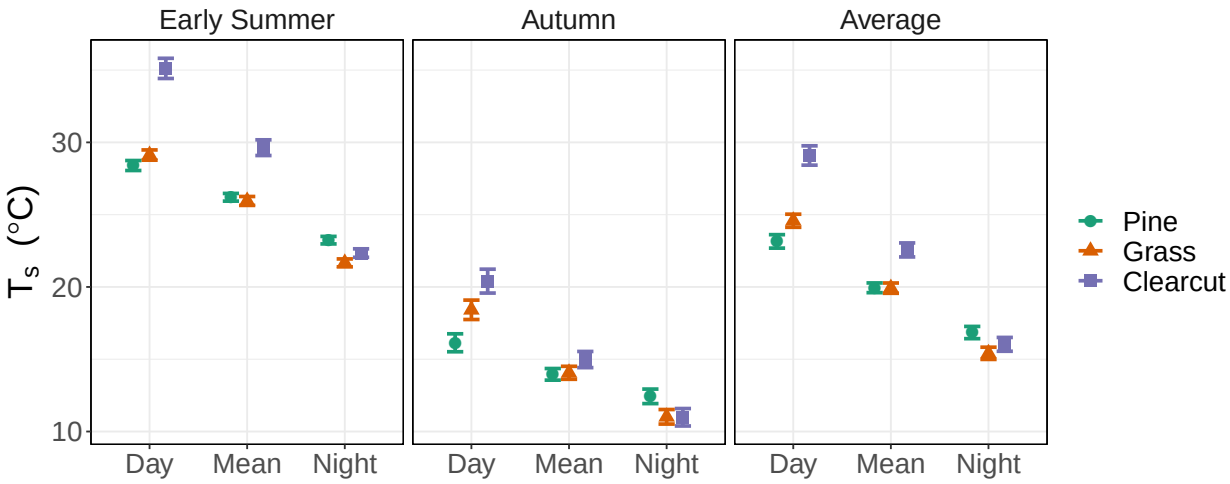

Figure 2.1: Mean daily, daytime, and nighttime surface temperatures for early summer (May, June), and August (October, November). Error bars represent plus or minus three standard errors of the mean. Units are in degrees Celsius.

The average daily T_s differed between two periods with contrasting patterns in vegetation structure. In the early summer, the switchgrass had full canopy coverage and a height of two meters (Figure: 2.4a). In contrast, after the harvest in the autumn, the switchgrass canopy coverage and height were very low (10 cm in height). The height and presence of vegetation at the Clearcut and Pine sites were constant through the measurement period, with the Clearcut lacking vegetation and the Pine full maintaining canopy coverage.

In early summer, while the switchgrass was actively growing, the Clearcut had much higher T_s than both Pine and grass, while differences between Pine and Grass were small. Daily average T_s at the Pine and Grass sites was only 0.3 °C different. The Clearcut site

was 3.7-3.4 $°C$ warmer than the Pine and switchgrass sites(Figure: 2.1). These differences were larger when examining only the daytime temperatures.

After the switchgrass was harvested in autumn, daily average T_s at all three sites were within $1°C$ of each other. During the daytime, Clearcut was $4.3°C$ warmer than Pine, and Grass was 2.3 $°C$ warmer than Pine. Clearcut and Grass were within 2 $°C$ of each other. Average nighttime T_s at Clearcut and Grass were approximately equal, with 10.9, and $11.1°C$, with the Pine stand being slightly warmer at 12.4 $°C$(Figure: 2.1).

To understand how temperatures fluctuate over the course of a day, we examined the mean diurnal course (MDC) of surface and air temperatures. Peak surface temperatures were highest at the Clearcut and lowest at the Pine tower, with the Grass tower intermediary (Figure 2.2). The Pine and Grass towers had similar surface temperatures in Early Summer, while Grass and Clearcut had similar temperatures in Autumn (Figure 2.2). Surface temperatures of all three towers re-converge at nigh-time. The air temperatures of all three towers are nearly identical; however the air temperature at the Pine tower was slightly lower between 0600 and 1800 (Figure 2.2). Pine averaged 1.4 $°C$ cooler than Grass and Clearcut in Early Summer, and 1.5 $°C$ cooler than grass, and 1.2 cooler than Clearcut in Autumn.

In addition to a reduction in maximum surface temperatures at the Pine stand, we also found a shift in the shape of the MDC of surface temperature, with peak temperatures occurring later in the afternoon at the Pine tower than at Grass or Clearcut. Furthermore, the surface and air diurnal temperature range (DTR) was similar at the Pine tower in Early Summer (9.9 and 10.0 $°C$) and Autumn (6.8, 6.4 $°C$), as well as the Grass tower in Early Summer (12.4 and 10.5). Overall, the Pine stand's surface temperature appears to be tightly coupled to the air temperature while the the Clearcut surface temperature is not. The surface temperature of the Grass field was only similar to air temperature in Early Summer.

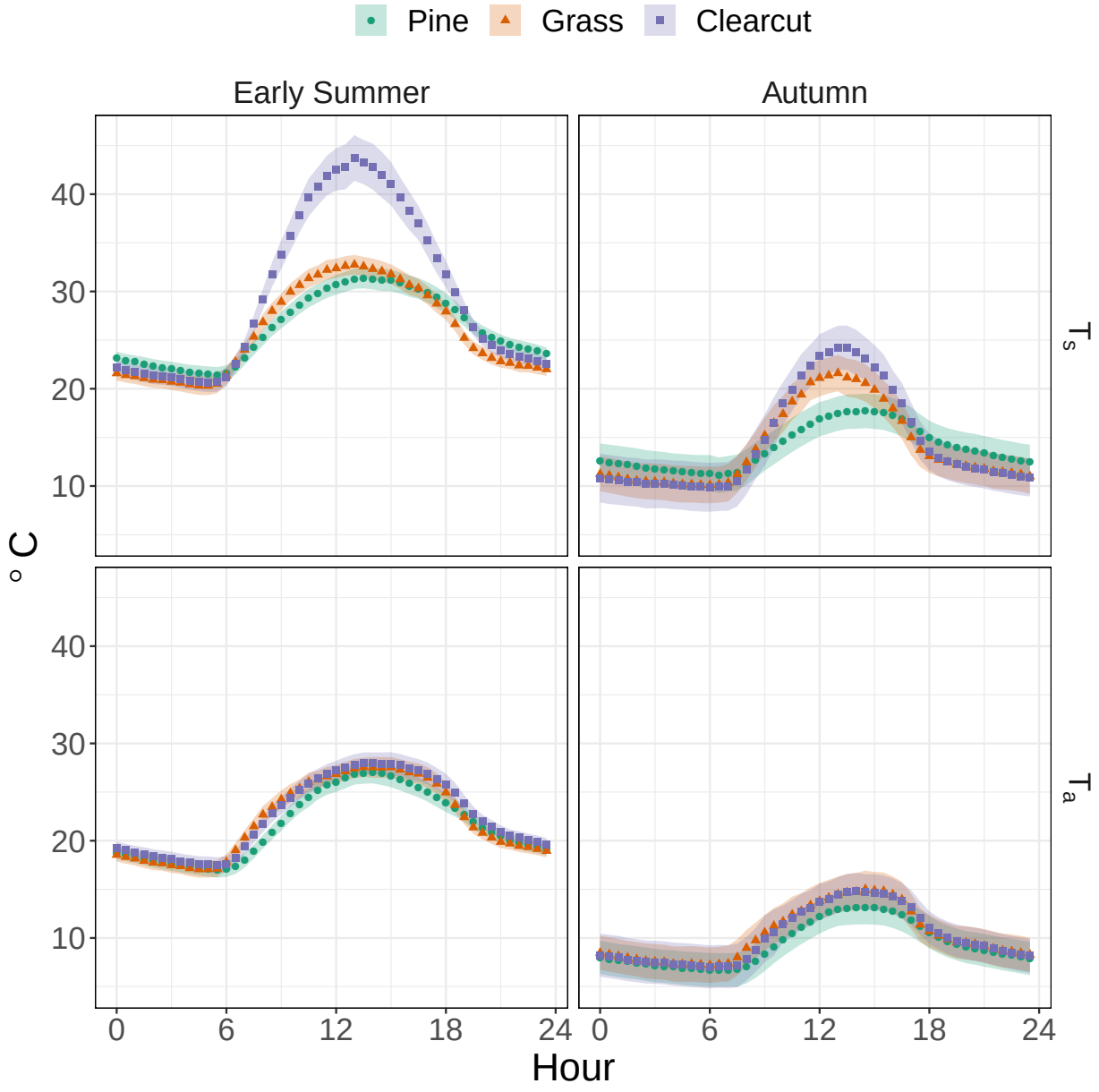

Figure 2.2: Mean diel surface and air temperature for early summer and autumn. Units are in degrees Celsius. Points are the mean value for the half hour, ribbons represent plus or minus two standard errors of the mean.

Table 2.1: Mean surface energy budget. Values are the annual mean for daytime fluxes. Units are in watts per square meter, ± two standard errors. S_i is incoming shortwave, S_o is outgoing shortwave, L_i is incoming long-wave, L_o is outgoing long wave, R_n is net radiation, LE is latent heat, H is sensible heat, G is ground heat flux. LE∗ and H∗ are the resulting latent and sensible heat fluxes if the energy balance was closed, maintaining Bowen ratio.

Site	S_i	S_o	L_i	L_o	R_n	LE	H	G	LE∗	H∗
					Early Summer					
Pine	429±15	42±1	401±1	446±1	342±13	191±8	75±5	9±0	239	93
Grass	416±15	83±3	399±1	450±1	280±11	187±7	51±3	11±1	212	58
Clearcut	423±15	74±3	401±1	489±3	255±10	65±3	115±5	29±1	82	144
					Autumn					
Pine	275±12	29±1	328±3	377±2	196±10	82±5	40±5	-3±0	134	66
Grass	265±12	58±3	325±3	391±2	143±8	47±3	57±5	4±1	62	76
Clearcut	265±12	51±2	323±3	401±3	134±7	46±3	71±5	9±1	49	76

2.4.2 Energy Fluxes and Mechanisms

To explore why surface temperatures differ among sites, we examined the energy budget of each ecosystem. Incoming short-wave and long-wave radiation was nearly identical among the three towers supporting the assumption that these systems share a background climate (Table: 2.1). Outgoing shortwave was lowest at the Pine tower and highest at the Grass and Clearcut. As a result, the albedo at the Pine was 0.1 higher than the Grass and Clearcut at both measurement periods (Table: 2.2). The combination of incoming and outgoing radiative fluxes resulted in the highest net radiation occurring at Pine (Table: 2.1). Grass net radiation was larger than Clearcut but more similar to Clearcut than Pine (Table: 2.1).

The increased net radiation at the Pine site was dissipated through an increase in sensible(H) or latent(LE) heat fluxes. Due to differences in energy balance closure, there is uncertainty directly comparing latent (LE) and sensible (H) heat fluxes among the three ecosystems. However, if we assume that H and LE are equally biased, we can examine how energy is distributed between these fluxes using the Bowen ratio (β). In early summer,

Pine and Grass were heavily weighted towards LE (low Bowen ratio), while Clearcut was dominated by H (Tables 2.1,2.2). In autumn, the Pine tower maintained a low Bowen ratio and the Clearcut maintained a high Bowen ratio. The Grass tower switched from a high Bowen ratio in Early Summer to a low Bowen ratio in Autumn. Friction velocity, a measure of atmospheric turbulence, was highest at the Pine tower, while Friction velocity at Grass and Clearcut were lower and very similar in Early Summer and Autumn (Table: 2.2). These observations suggest that the changes in surface temperature from Early Summer to Autumn at the Grass tower were due to Bowen ration changes and not albedo or differences in turbulence. Furthermore, during the Early Summer, the Pine and Grass ecosystems increase LE in response to elevated radiative inputs (Figure 2.3. The lack of a similar response in the Clearcut demonstrates how the lack of latent heat in the summer is an important driver of the elevated T_s

Table 2.2: Seasonal mean daytime friction velocity (u$*$), albedo (α;S_o/ S_i), Bowen ration(β; H/LE), and aerodynamic resistance (r_a) for the Pine, grass, and Clearcut towers. Units for u$*$ are in meters per second, α and β are unit-less, r_a is in s/m

Site	u$*$	α	β
Early Summer			
Pine	0.36	0.10	0.39
Grass	0.20	0.20	0.27
Clearcut	0.23	0.17	1.76
Autumn			
Pine	0.46	0.11	0.49
Grass	0.25	0.22	1.22
Clearcut	0.26	0.19	1.55

2.5 Discussion

Prior observational research comparing land surface temperature changes associated with reforestation has focused on differences between a low stature vegetated system (grassland) and forests (Lee et al., 2011) (Zhang et al., 2020). Here, using a unique site with three co-located flux towers that include two vegetated and one non-vegetated system, we found that the differences between the vegetated ecosystems were minor compared to the differences between the bare-ground clearcut and the two vegetated systems (Pine and Grass). This indicates that the moderate influences of reforestation on surface temperature in the temperate region that others have reported may not capture the full influence of land-cover

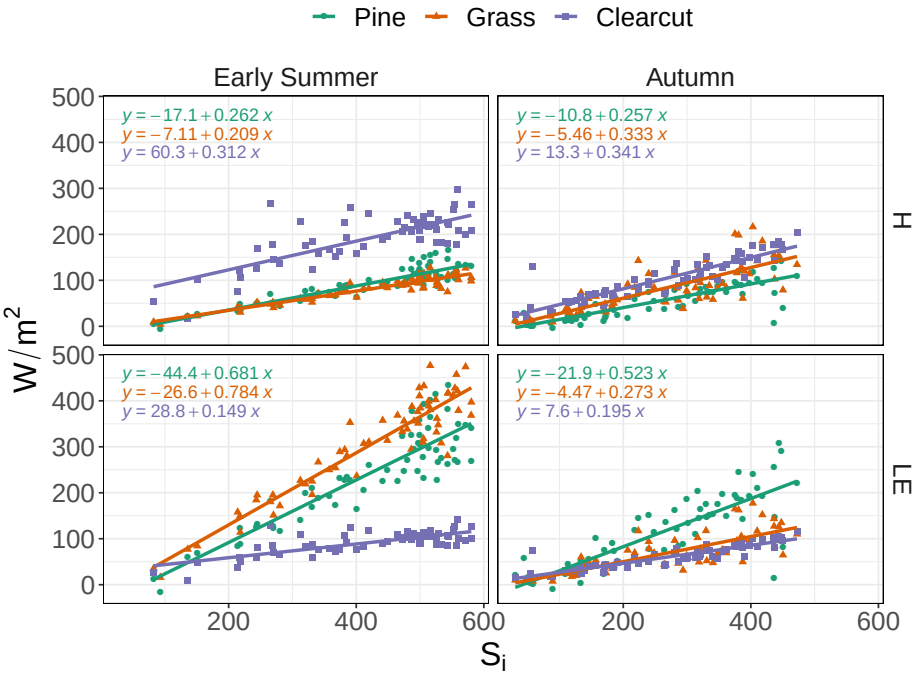

Figure 2.3: Mean daytime sensible (H) and latent (LE) heat flux as a function of incoming shortwave radiation (S_i), for early summer (May, June), and August (October, November). Lines represent the best fit for a linear model with the model displayed in the top right of each panel. Equation order from top to bottom is Pine, Grass, Clearcut. Units are in W/m^2 for H and LE, and °C for air temperature. H and LE used in this graph are corrected for energy balance closure

change on surface temperature (Lee et al., 2011) (Zhang et al., 2020). While the bare-ground state is temporary in a harvest and recovery cycle, we observed that these bare-ground periods could have major influences on the change in surface temperature associated with a land-cover change decision.

When aggregated across the growing and dormant seasons, we found that conversion from Grass to Pine to result in no change in average surface temperatures and air temperatures as in previous work (Lee et al., 2011). However, we found that differences were observed during the daytime that varied seasonally. When the Grass system was actively growing in the early summer, Pine and Grass daytime T_s were nearly identical. After the switchgrass was harvested, removing vegetation, there was very little difference between the Grass T_s and the Clearcut T_s. This implies that the presence of vegetation can affect T_s. We included the Clearcut tower in this analysis to directly compare the effects of vegetation, regardless of height, on T_s. We found that clear-cutting a pine plantation resulted in large T_s differences greater than 4 $°C$. These differences are much larger than the pine-grass comparison from this study and previous works. While we found that forest temperatures are slightly warmer at night when assuming 0.95 emissivities for each system, this conclusion is not robust to changes in the emissivity assumption used to calculate T_s and the alternative temperature metrics used in the analysis. (Figure:2.5). The large temperature difference between two short ecosystems, one vegetated and the other bare ground, combined with the small temperature difference between two vegetated ecosystems with large differences in height, allowed us to make an inference as to the mechanism of T_s change.

We found that latent heat flux was the essential mechanism explaining the change in T_s. As solar radiation increased during the growing season, an increase in the latent heat flux could dissipate the energy in the pine and grass ecosystem, but not in the non-vegetated clearcut. The lack of latent heat flux at the clearcut forces energy to be dissipated via sensible

heat. Without the increased sensible heat, T_s would be even greater at the clearcut site. Previous work using other eddy-covariance sites has determined that a change in surface resistance is the primary mechanism governing surface temperature differences (Burakowski et al., 2017, Lee et al., 2011, Rigden and Li, 2017)). These studies used attribution models to assign the relative temperature difference to differences in albedo, surface resistance, and Bowen ratio. These same models did not produce reliable results at our site because the predicted temperature differences between sites did not match the observed temperature differences (Appendix 2A). This study focused on examining the direct changes in albedo, friction velocity, and Bowen ratio to evaluate mechanisms. We show differences in friction velocity between the three ecosystems, but these differences do not change seasonally despite the observation that the relative temperature differences between the sites change seasonally (Table: 2.2). However, Bowen ratio and LE did change seasonally. When the T_s differences between Pine and Grass were smallest, the Bowen ratio and the response of LE to S_i were similar. The biggest difference between the vegetated and non-vegetated ecosystems in early summer was how much energy was distributed into LE (Figure: 2.3. By including the bare-ground system for comparison, the importance of LE in temperature regulation during the summer is clear from direct observations.

Our results match more closely with remote sensing studies than with other eddy covariance based analyses. For example, Mildrexler et al. (2011) found that air and surface temperatures at forested sites were strongly related, while air and surface temperature at barren sites were less related. They also found that the ability of forests to maintain evapotranspiration was the primary mechanism of reduced surface temperatures. However, they found that crops and grasses globally have higher T_s than T_a. Here we show that a bioenergy crop has similar air and surface temperatures during the growing season. This disparity may resolve during periods of water stress not present in our observations. Alternatively, the

switchgrass used in our study may have higher rates of evapotranspiration to support high yields than the grasses included in Mildrexler et al. (2011).

Changes in T_s result from a change in energy balance and is an important state variable for climate models and is a key factor regulating biological processes at the surface (Bonan, 2008a, Jackson et al., 2008, Juang et al., 2007). However, changes in T_s do not result in changes to global temperature. As discussed above, latent heat flux reduces T_s but this energy is released when the water vapor condenses elsewhere. Furthermore, changes in albedo and atmospheric carbon dioxide concentration resulting from land cover change can affect global temperature and energy balance. Consequently, afforestation has been shown to decrease T_s but increase upper atmosphere air temperatures Winckler et al. (2018). To understand the total climate forcing resulting from a land cover conversion, both the local and global effects need to be considered.

In summary, we found that vegetated ecosystems, regardless of height, reduced surface temperature compared to a bare-ground ecosystem. This reduction in T_s was primarily due to the vegetated ecosystems capacity to transfer energy away from the surface using latent heat flux. As a result, ecosystem management for surface climate mitigation in the temperate region may benefit from primarily focusing on the presence of vegetation throughout the year rather than a specific ecosystem type.

2.6 Appendix 2A: Data Coverage and Phenology

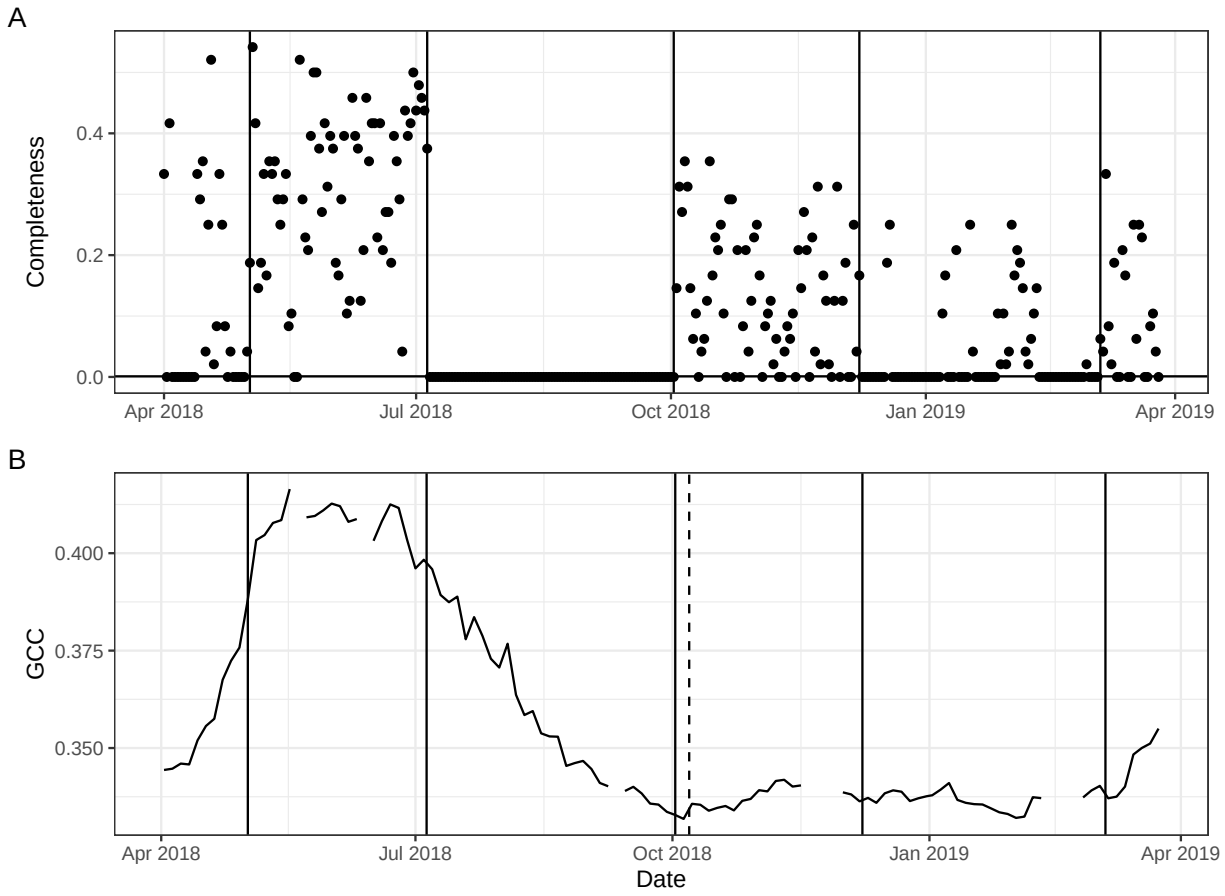

Figure 2.4: The overlap between periods of time with good data coverage and key switchgrass phenological phases. A) Daily average energy balance completeness for all three towers, solid vertical lines indicate the beginning and ending of consistent data outage periods. B) Green Chromatic Coordinate (GCC) of the Grass tower during the observation period. Solid vertical lines are the same dates as A, the dashed vertical line represents when the Grass field was mowed.

2.7 Appendix 2B: Sensitivity to Emissivity and Temperature Metric

In the main text, surface temperature was calculated from the measured outgoing longwave radiation using the Stephan-Boltzman relationship (Equation 2.1). Therefore changes in surface temperature among the three towers are sensitive to the emissivity (ϵ) used in this equation. Emissivity is difficult to measure *insitu*; determining T_s requires making assumptions regarding emissivity. We tested the sensitivity of our results to two different assumptions of emissivity. The first assumption was that emissivity did not vary with time or ecosystem type. We used the ecostress emissivity product to determine our site's constant emissivity value (Hook and Hulley, 2019). The second assumption was that emissivity varied with time and ecosystem type. Other land surface temperature studies have assumed that emissivity was related to albedo Juang et al. (2007). We followed Juang et al. (2007) to calculate a dynamic emissivity product from albedo values.

Additionally, T_s' appropriateness as a metric for climate services can be questioned (Novick and Katul, 2020). However, the actual air temperature measured at any particular location may not be directly connected to the land-cover at that location. (Novick and Katul, 2020) proposed an aerodynamic temperature as an alternative land-cover change temperature metric. We followed their method to derive aerodynamic temperature from observations and compared the two temperature metrics.

Overall, we found that the exact differences of T_s among the three ecosystems depended on the temperature metric and emissivity assumption. However, each temperature metric showed that Clearcut has the highest temperature, Pine had the coolest, and the Grass was intermediate (Figure 2.5. The seasonal patterns described in the results was also maintained, with small Pine-Grass differences in early summer and small Grass-Clearcut dif-

ferences in autumn. Nighttime temperature differences were minor when constant emissivity is assumed, but both alternative metrics show almost no nighttime temperature differences. Therefore, we do not have adequate evidence to confidently state that there are differences in nigh-time temperature among these three ecosystems.

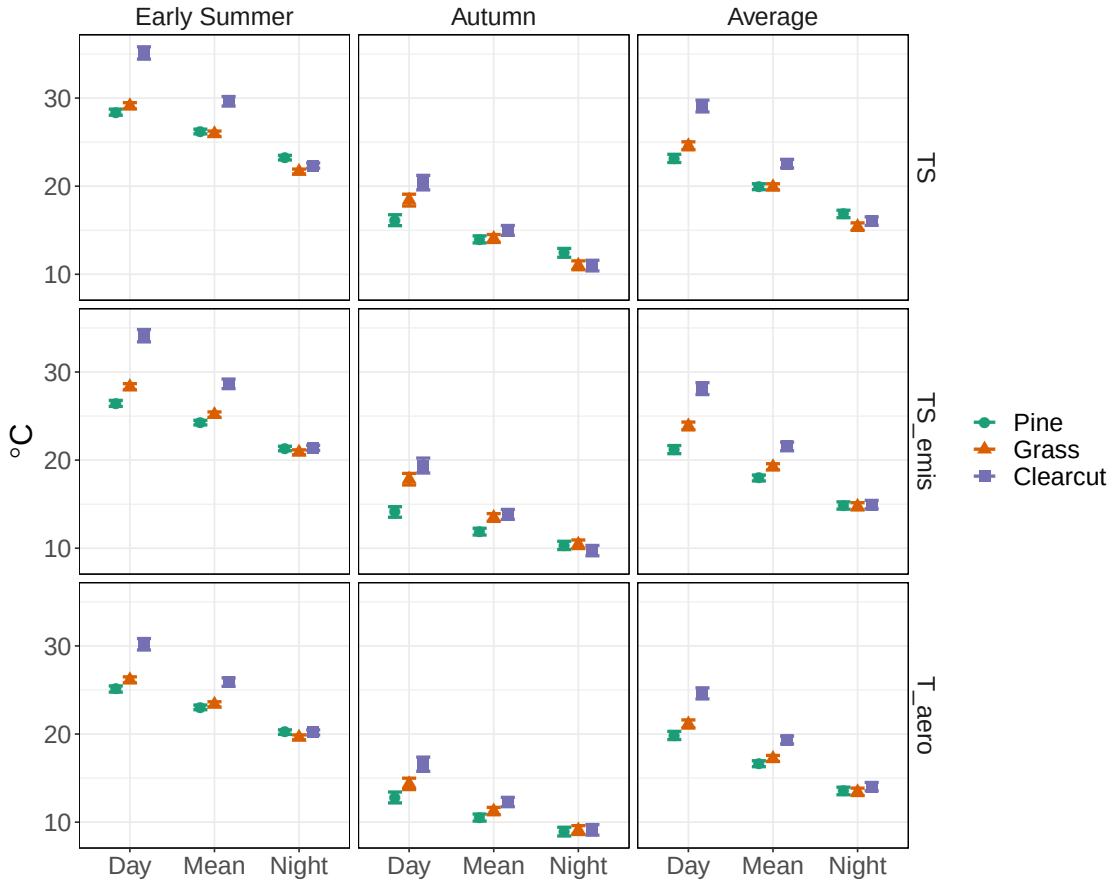

Figure 2.5: Seasonal and average temperature metrics for day, night, and average. TS is surface temperature, identical to Fig(2.1). TS_emis is surface temperature calculated using variable emissivity, which is a function of albedo as in Juang et al. (2007). T_aero is the aerodynamic temperature, calculated as in Novick and Katul (2020). For both Ts_emis, and T_aero, there are no nighttime temperature differences between systems, while daytime temperature differences do not differ substantially from TS. At this site, nighttime temperature differences are negligible and subject to different emissivity assumptions and temperature metrics. Daytime differences however, are large and consistent.

2.8 Appendix 2C: Attribution of Surface Temperature Change with the Intrinsic Biophysical Mechanism

When studying LCC effects on T_s it is important to understand the mechanisms responsible for differences among ecosystems. To this end, attribution metrics have been developed based on the decomposition of the surface energy budget. One of the first papers to use this method was Juang et al. (2007). Juang et al. used the surface energy balance equation and linearized using Taylor series expansion to attribute temperature change directly to a change in aerodynamic conductance, albedo, ground heat flux, and emissivity. This method was adapted by Lee et al. (2011) to be more general, creating the intrinsic biophysical mechanism (IBM) method, which attributes ΔT_s to changes in albedo, Bowen ratio, and surface roughness. Subsequent metrics have been developed, but all of them are based on the IBM method (Bright et al., 2017, Burakowski et al., 2017, Chen and Dirmeyer, 2016, Liao et al., 2018, Luyssaert et al., 2014, Rigden and Li, 2017).

Here we used the IBM method based on Lee et al. (2011) for simplicity and comparability to prior studies. We found that the IBM method correctly predicted the sign and was roughly the correct magnitude for daytime ΔT_s (Figure 2.6). However, the predicted ΔT_s did not closely match the observed ΔT_s, particularly in autumn. We attempted the same analysis with the different version of the IBM method cited above (i.e., including ground heat flux) and altered the time-scale of analysis to minimize energy balance closure issues. None of the modifications produced results that improved on the original IBM method. Therefore we concluded the IBM method was not suitable for discerning the mechanisms explaining the differences in T_s at this site and focused the main text examining direct differences in albedo, Bowen ratio, and friction velocity.

There are multiple reasons why the IBM method failed at matching the observed

temperature differences. First, the IBM method implicitly excludes nighttime data. We do not present nighttime data because there was not enough data left after the implicit filtering to conduct an analysis. The IBM method calculates surface roughness based on the resistance concept and inverts resistance from sensible heat flux. The sensible heat flux observed here is negative at night after the nocturnal inversion. Lee et al. (2011) cited this as a possible explanation for the higher night-time temperatures of forest ecosystems. However, negative sensible heat flux would result in negative resistance in the IBM calculations, which is physically impossible and therefore meaningless. During the day, the same error occurs though, to a lesser degree. Negative sensible heat flux observations during the day are less common but are still implicitly filtered out of the data set. In addition, periods of near-zero sensible heat flux, such as dawn and dusk, results in a surface resistance greater than 1000 $ms^{-}1$, again physically impossible. This implicit filtering eliminates observations of low or negative sensible heat flux, resulting in a sampling bias leading to possible overestimation of the role of surface roughness/resistance. Second, the Taylor series expansion surrounding air temperature may reduce the accuracy of the IBM method. In any linearization of the energy balance equation that includes the term T_s, T_s must be replaced with an approximation since T_s is what the method is solving. This is done by approximating T_s with T_a. First-order Taylor series expansions are adequate when the two values are close, but the approximation is less accurate when the differences are large, as we see between the Clearcut. Chen et al. (2020) found that adding in second-order terms improved model fit but did not alter the findings using only first-order terms significantly and required increased calculation costs. In other studies of only vegetated ecosystems, the difference in T_s with T_a was slight; therefore the error associated with this approximation is small. In our study, T_s and T_a were nearly identical at the Pine stand, but very different at the Clearcut (Figure 2.2).

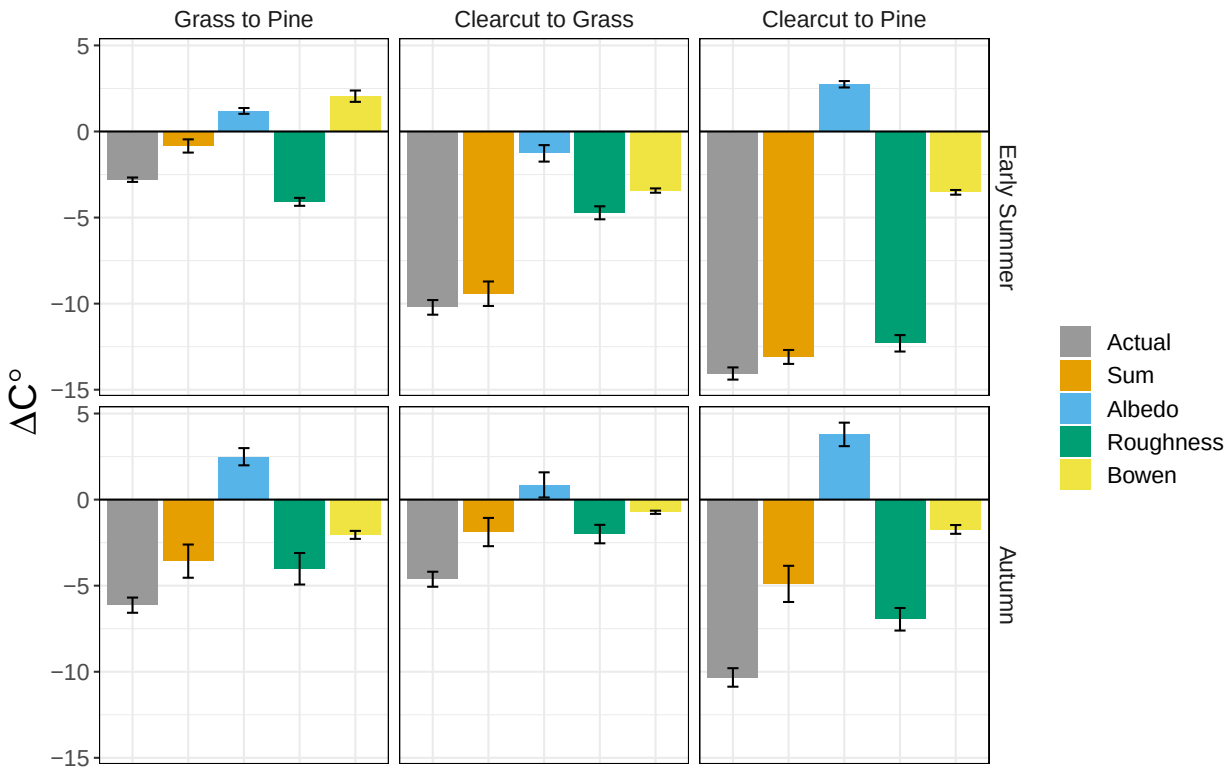

Figure 2.6: Observed and modeled changes in surface temperature for three land-cover conversions, Grass to Pine, Clearcut to Grass, and Clearcut to Pine. Bar heights represent the mean daytime average change in surface temperature, whiskers represent 3 standard errors of the mean. Grey bars are derived from observations, colored bars represent the mechanisms of surface temperature change and the total of these processes, calculated using the intrinsic biophysical mechanism (IBM) method (Lee et al., 2011).

Chapter 3

A minimally managed switchgrass ecosystem in a humid subtropical climate is a source of carbon to the atmosphere

3.1 Abstract

Bioenergy has been identified as a key component of climate change mitigation. Therefore, quantifying the net carbon balance of bioenergy feedstocks is crucial for accurate projections of climate mitigation benefits. Switchgrass (*Panicum virgatum*) is a model bioenergy crop with high yields, low maintenance, deep roots, and strong carbon sequestration potential. However, assessments of net annual carbon exchange between switchgrass fields and the atmosphere are rare. Here we present net carbon fluxes of a minimally managed switchgrass field in Virginia (Ameriflux site US-SB2) during the third, fourth, and fifth-year since establishment. Cumulative net ecosystem exchange (NEE) of carbon was 239 g C m^{-2} (193, 290; 95% confidence interval) over the entire observational period. Annual totals were 201(172, 229), -74(-101, -47), and 113(82, 144) g C m^{-2} yr^{-1}, for the first, second, and third year of observation. When accounting for the amount removed during harvest, the net ecosystem carbon balance (NECB) was 327, 220 and, 369 g C m^{-2} yr^{-1} respectively, indicating a consistent carbon source to the atmosphere. This differs substantially from other studies showing switchgrass to be either neutral or a sink of carbon. This study illustrates that predictions of net carbon climate benefits from bioenergy crops can not assume that the ecosystem will be a net sink of carbon from the atmosphere. Background climate, management, and land-use history may determine whether widespread deployment of switchgrass as a bioenergy feedstock results in realized climate change mitigation.

3.2 Introduction

Carbon dioxide (CO_2) concentrations continue to rise in the atmosphere, primarily due to fossil fuel combustion (IPCC, 2013). One possible method of reducing CO_2 emissions is to replace fossil fuels with bioenergy (Pacala, 2004). Bioenergy crops absorb atmospheric CO_2 to create biomass, some portion of which is harvested and used as fuel. In perennial bioenergy crops, the above-ground biomass is harvested and processed into fuel, while the below-ground components remain on site. Therefore, perennial biofuel crops have the potential double benefit of offsetting CO_2 emissions by preventing fossil fuel combustion and sequestering carbon below ground. (Adler et al., 2007, Anderson-Teixeira et al., 2013).

Switchgrass (*Panicum virgatum*) has emerged as a promising bioenergy feedstock for the United States (Wright, 2007). Switchgrass is a fast-growing, perennial, C4, grass species that is native to North America. It can have high yields (above-ground biomass) and is well-suited to various climate conditions (Parrish and Fike, 2005, Wright, 2007). Furthermore, switchgrass has high below-ground biomass as well, enhancing the potential to sequester carbon from the atmosphere into below-ground pools (Parrish and Fike, 2005, USDA-Natural Resources Conservation Service, 2011). It has low fertilizer and pesticide requirements and is compatible with conventional farming equipment (Wright, 2007). Sustained high yields of switchgrass biomass require less than 50 kg N ha^{-1} per year, but many studies have shown sustained yields with no nitrogen additions (Parrish and Fike, 2005).

While the production of high yields with few management inputs is important for a bioenergy crop, yields alone do not fully represent the crop's climate mitigation potential because they does not represent the full carbon balance of the bioenergy ecosystem (O'Halloran and Bright, 2017). The net carbon balance of a bioenergy feedstock includes the non-growing season carbon fluxes and the carbon stored below ground. Therefore, field

scale, year-round observations of CO_2 exchange with the atmosphere are required for a full accounting of the carbon balance of the bioenergy ecosystem.

Eddy covariance (EC) is a widely used method for measuring the net ecosystem exchange (NEE) of CO_2 between terrestrial ecosystems and the atmosphere at the field scale (Baldocchi, 2014). However, only a few studies have used EC to study the carbon balance of bioenergy switchgrass systems, most of which found switchgrass to be a carbon sink on annual time scales. Skinner and Adler (2010) studied a switchgrass field in Pennsylvania for four years, finding a net sink the first three years and a source the fourth year. Zeri et al. (2011) examined multiple bioenergy crops, including switchgrass, in central Illinois for 2.5 years and found switchgrass to be sink over the whole observation period. Wagle and Kakani (2014) used EC to study two and three-year-old switchgrass stands in Oklahoma and found switchgrass to be either a small sink or small source depending on the climate conditions. However, their measurements were limited to the growing season, excluding any potential respiration fluxes during the dormant season (Wagle and Kakani, 2014). Eichelmann et al. (2016a) used EC to study a mature switchgrass (6th and 7th year) field in Ontario, Canada for two years and found that switchgrass can alternate between sink and source depending on the climate conditions. Di Virgilio et al. (2018) studied switchgrass using EC during the first 4 years of establishment in the Po River Valley in Northern Italy and found switchgrass to be a strong sink each year, even including harvested carbon. Finally, Abraha et al. (2018) used EC to study two switchgrass fields for eight years following establishment in Michigan and found that the switchgrass field's carbon balance depended on the previous land-use. In particular, switchgrass planted on former agricultural land was a carbon sink, while switchgrass planted on former conservation grassland was a minor source.

Switchgrass plantations appear to be most commonly a net sink of carbon, with some effects due to age and the legacy effects from the previous land-use. However, with

the existing small sample size, it is difficult to generalize. The majority of these studies were limited to the first years of switchgrass establishment and included annual nitrogen fertilization as part of crop management. Furthermore, they have coincidentally sampled a narrow window of climate space, with studies ranging from cool and wet to hot and dry, but with only one study in a cool and dry environment and no previous studies in warm and wet climates (Figure 3.1).

This study seeks to address the need for EC studies of switchgrass in minimally managed (non-fertilized) fields within a warm and humid climate. Our site in central Virginia, USA, complements prior studies that were largely in cooler or drier climates (Figure 3.1), and were fertilized at higher rates. We present three years net ecosystem exchange (NEE) observations, peak biomass, baled yields, and the net ecosystem carbon balance (NECB) during the third, fourth, and fifth year of switchgrass establishment following con-

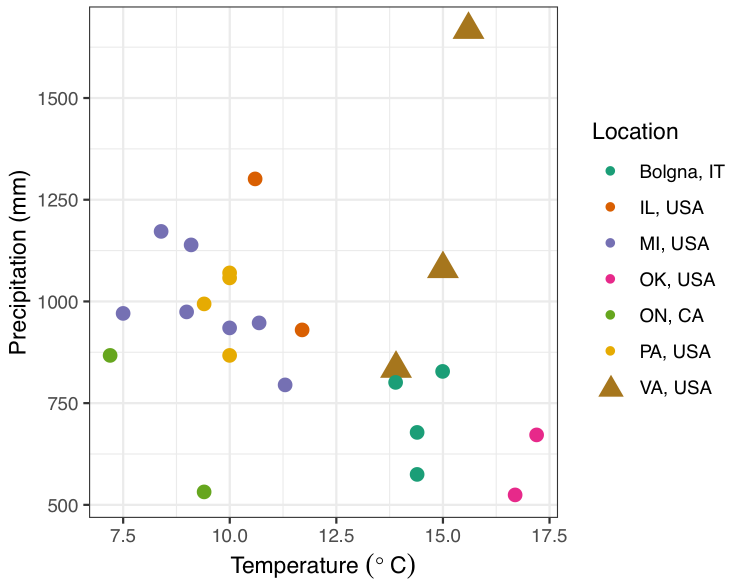

Figure 3.1: Climatic conditions (mean annual precipitation vs. mean annual temperature) from published switchgrass eddy-covariance studies. Data for US-SB2 in VA, USA (this study), ON,CA (Eichelmann et al., 2016a), PA,USA (Skinner and Adler, 2010), OK,USA (Wagle and Kakani, 2014), IL,USA (Zeri et al., 2011), Bolgna,IT (Di Virgilio et al., 2018), MI, USA (Abraha et al., 2018).

version from a perennial grass field used for hay production.

3.3 Methods and Materials

Site characteristics

We deployed an eddy covariance system in March 2016 over an 8.4 hectare switchgrass field located on Sweet Briar College's campus in central Virginia (37.5605 N, -79.0884 W, elevation 240 m) as part of the Sweet Briar College Land Atmosphere Research Station (SBC-LARS). The site is registered in the Ameriflux Network as US-SB2. An upland cultivar of switchgrass (Blackwell) was sown in June 2014 in a field previously used for hay production. The seed mixture included a micro-nutrient blend, but no further fertilization was applied in subsequent years. Mowing, bailing, and harvest removal occurred in the late summer to autumn of each year (Table 3.1).

Table 3.1: Timing of major switchgrass phenology and management events for the field in Central Virginia

Event	2016	2017	2018
Emergence	April 18	March 21	April 23
Sampling	August 18	July 21	July 27
Cutting	September 11	August 20	October 7
Removal	October 7	August 23	October 24
Dormant	November 11	November 13	November 15

This regions climate is humid subtropical (Köppen climate classification Cfa), with warm-humid summers and cool-mild winters. Temperatures over the period of observation were approximately equal to the 30-year average (Table 3.2). Precipitation varied substantially across the three study years, with near-average precipitation in 2016 (1080 mm), below average in 2017 (836 mm), and record-high precipitation (1669 mm) in 2018 (Table

3.2); partially due to 64 mm of rainfall associated with Hurricane Florence in September (Stacey Stewart and Robbie Berg, 2018). The soil is Clifford clay loam and Wintergreen clay loam, both severely eroded soils with very small organic horizons.

Table 3.2: Monthly temperature and precipitation for 2016 - 2018 and the 30 year monthly averages from the nearest weather station to US-SB2 (Lynchburg, VA).

Temperature (C °)						Precipitation (mm)					
Month	Average	2016	2017	2018	2019	Month	Average	2016	2017	2018	2019
January	2.5		4.2	0.6	2.1	January	81.8		84.6	74.7	71.9
February	3.9		8.3	6.9	5.7	February	71.6		15.2	145	123
March	8.1		8.6	5.3	6.8	March	93.2		60.7	78	90.4
April	13.6	13.1	16.1	11.7		April	79.2	53.8	106	122	
May	18.1	17.2	18.1	21.7		May	90.7	175	200	211	
June	22.8	22.5	21.9	23.6		June	95.5	159	53.1	123	
July	24.7	25.3	26	24.7		July	106	152	82.6	147	
August	23.9	25.3	23.3	24.2		August	94.7	30.2	56.9	113	
September	20.3	22.5	20	22.5		September	89.7	85.9	48.5	172	
October	14.2	16	15.6	15.3		October	78.2	43.9	65.3	121	
November	8.6	9.7	7.8	6.4		November	76.7	29.7	25.9	151	
December	3.6	3.6	3.1	4.2		December	78.2	78.7	17.5	181	
Average	13.6	14.2	14.3	13.9		Sum	1036	1080	836	1669	

Flux Measurements

Flux measurements began on March 26, 2016, using the eddy covariance (EC) method. Here we use data covering the first three years of observation ending March 25, 2019. The EC instruments were mounted at 4 m above ground level and included a sonic anemometer (Gill Windmaster Pro, Gill Scientific) and a closed path infrared-gas analyzer for measuring CO_2 and H_2O gas concentrations (Licor 7200, Licor Environmental). Data were collected continuously at 10 Hz and averaged at 30 minute time intervals using EddyPro version 6.2.2 (LI-COR, Inc., 2019). We implemented a double-rotation method to account for tilt in the anemometer, a block average detrending method, and compensation for density fluctuations.

Quality checks were performed according to (Foken et al., 2004). Raw data was screened for spikes, amplitude resolution, drop-outs, absolute limits, skewness, and kurtosis according to (Vickers and Mahrt, 1997). Footprint estimation was performed according to (Kljun et al., 2004). Because this footprint model depends on canopy height, we supplied a dynamic height file to the EddyPro software that describes switchgrass's changing height. Height was determined by visually inspecting PhenoCam images (Seyednasrollah et al., 2019), using a vertical PVC pipe in the field, marked every 10cm from the ground up to two meters. We did not include an angle of attack correction, as the available correction includes artificial inflation of the vertical wind measurement (LI-COR, Inc., 2019). We use the meteorological sign convention where negative fluxes indicate flux downward towards the ground (i.e. negative NEE indicates carbon sink into the ecosystem).

We applied a two-part spatial filter to the half-hourly fluxes to limit the influence of observations that do not represent the switchgrass field. First, we used the flux footprint model estimations (Kljun et al., 2004) to identify where the cumulative normalized contribution to the flux footprint equaled 70%, and we removed any observations where the distance and direction of the 70% footprint fell outside of the switchgrass field. Second, we removed all fluxes originating from the north quadrant (above 315°and below 45°) due to potential contamination from a brush pile at a range of 145 m. We also removed unrealistic NEE observations beyond -50 and 50 μmol m^{-2} s^{-1} and observations beyond 3 standard deviations of a 30-day running mean.

To remove data with inadequate turbulence, we applied a friction velocity (u^*) filtering routine. This method removes observations where u^*falls below a calculated threshold, indicating that fluxes cannot be calculated using the eddy covariance method. We determined the u^*threshold by examining the relationship between $u^*$and NEE fluxes as in Papale et al. (2006) using the REddyProc R-package (version 1.2) (Wutzler et al., 2018). The final

data coverage after all of the filters were applied was 37.4%. While the data coverage is low, this amount of filtering was required to ensure that the reported results represent the switchgrass in this small field.

To obtain annual and seasonal totals of NEE, we filled the gaps resulting from measurement interruptions or filtering with modeled values using the REddyProc R-package (version 1.2) marginal distribution sampling algorithm (Reichstein et al., 2005, Wutzler et al., 2018), a widely-used approach. This method utilizes the co-variation of fluxes with meteorological variables and the temporal auto-correlation with the time of day. Gaps are filled by applying averages derived for a specific time of day, time of year, and meteorology.

To partition observations of NEE into gross primary production (GPP) and ecosystem respiration (RE) fluxes we applied the REddyProc R-package (version 1.2) implementation of the Reichstein partitioning method (Reichstein et al., 2005, Wutzler et al., 2018). The method uses nighttime data, when fluxes from photosynthesis are not present, to estimate the relationship between measured fluxes and air temperature. This relationship is then used to calculate daytime respiration fluxes using daytime air temperature observations. GPP is calculated as the difference between observed NEE and modeled RE. For more detail on this algorithm, see Wutzler et al. (2018).

Uncertainty Estimation

We estimated the uncertainty in NEE attributable to the u*threshold estimate by calculating two additional threshold estimates using the ReddyProc R-package algorithm (Wutzler et al., 2018). Revised estimates of the u*threshold were calculated by bootstrapping the observations within each season, resulting in a range of possible u*threshold estimates. We extracted the 5th and 95th percent quantiles of this threshold range in addition to the stan-

dard u*threshold. We applied these multiple u*filters to our data as previously described and examined the effect on cumulative annual sums of NEE.

We estimated the gap-filling and observational uncertainty of each observation and its effect on annual cumulative sums of NEE. We assessed these source of uncertainty by making 1000 random draws for each half-hour observation from a representative distribution. For half-hours that were gap-filled, this was based on a normal distribution centered on the estimated flux, with the standard deviation based on the variation resulting from different sized windowing within the REddyProc gap-filling algorithm (Wutzler et al., 2018). For non-gap-filled observations, the Laplace distribution was used based on (Aubrecht et al., 2016), where the distribution is centered on the observed flux, and the spread increases with the flux magnitude. This resulted in 1000 randomly distributed flux estimates for each half-hour that were averaged to the daily time step and summed over the whole time series, within observation year and seasonally.

Energy balance closure

We used energy balance closure (EBC), to asses the accuracy of our eddy covariance measurements. EBC is calculated by comparing the sum of the turbulent heat fluxes (sensible(H) and latent heat (LE)) to the net radiation (longwave, shortwave, and ground heat flux). Our 30-minute average EBC for the full observation period was 67%. This EBC is not ideal but close to the typical range EC of studies globally 80% (Foken, 2008, Twine et al., 2000). No corrections were applied to NEE fluxes reported here as a lack of EBC closure could result from errors in radiation measurements or from neglecting heat storage in biomass.

Biomass Sampling

Sampling of above-ground biomass occurred August 18, 2016, July 21, 2017, and July 27, 2018. All randomly located 1 m^2 quadrats within the flux footprint were cut to a height of 5 centimeters. Nine samples were taken in 2016, 14 in 2017, and 15 in 2018. Sampling dates were as near as possible to peak biomass, estimated from the Phenocam. Samples were stored in air-permeable paper refuse bags and dried at $50/degreeC$. Dry weights were measured using a calibrated lab scale. Results from our sampling are reported as "peak" biomass. Official yield numbers were measured by the baler during baling and reported by the harvesting company on a per-field basis, reported here as "removed".

Phenocam and Season Determination

To track the development of the switchgrass independently of the flux measurements we installed a web camera connected to the PhenoCam network (Seyednasrollah et al., 2019) under the site name "sweetbriargrass". This webcam captures standard RGB images and uploads them to the PhenoCam server every 30 minutes. Per standard PhenoCam network methods (Seyednasrollah et al., 2019), we calculated a green chromatic coordinate (GCC) for the switchgrass pixels in the image by dividing the green layer by the total of all three layers such that:

$$GCC = \frac{Green}{Green + Red + Blue}$$

Seasons were determined using this GCC product. Emergence was defined as the first day that GCC exceeded 0.36 within that year. The start of the post-harvest season was defined by when the field was mowed. The dormant season was determined as the first day the GCC declined below 0.34 after the secondary growth and ended on the first day of the following years growing season.

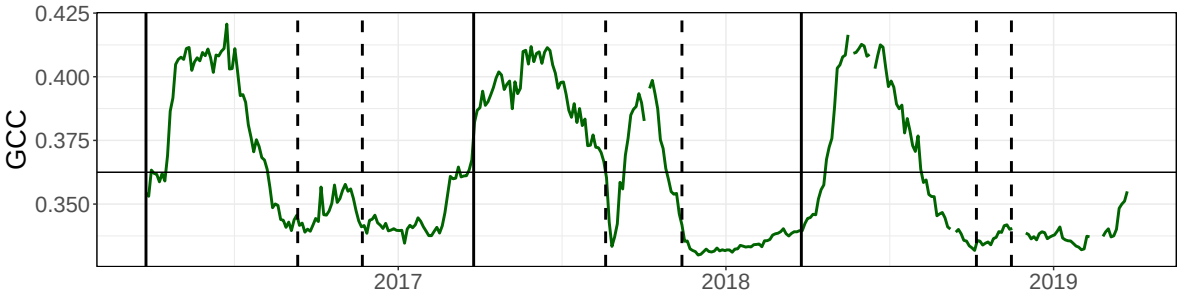

Figure 3.2: Green chromatic coordinate (GCC) for 2016 - 2019 from the Phenocam located at the field. Solid vertical lines indicate the start of the observation year. Dashed vertical lines indicate when the field was mowed (first line within a calendar year) and when the field becomes dormant (second line within a calendar year)

3.4 Results

Phenology and Seasonal NEE

The temporal dynamics of NEE strongly reflect the seasonal phenology of a perennial grass crop. In our first observation year, emergence occurred on April 18, 2016 (Figure 3.2, Table: 3.1). Daily NEE was negative for the first time during the first measurement year on May 14, 2016, following a brief period of CO_2 release to the atmosphere, likely due to mowing that occurred immediately before the EC system installation (Figure 3.3). Carbon sequestration peaked at -8.6 gC m^{-2} day^{-1} on May 30th, 2016. The field became a source of CO_2 to the atmosphere on July 18, 2016 and the magnitude of the CO_2 release increased until August 14, 2016. The release of carbon peaked at 10.3 gC m^{-2} day^{-1} on July 4th, 2016 however, the 14-day average NEE did not peak until September 25th, at 5.7 gC m^{-2} day^{-1} (Figure: 3.3). The magnitude of the CO_2 release began to decrease and approach zero after August 14, likely due to increasing photosynthesis from regrowth under the canopy. The switchgrass was mowed and raked into rows on September 11, 2016. However, due to rain and unpreventable logistical delays, baling and removal did not occur for another 26 days on October 7, 2016. This led to a large release of CO_2 to the atmosphere and the least efficient conversion of

peak biomass to baled yields among the three study years (Table: 3.3). NEE decreased into the dormant season, which began on November 22, 2016. The dormant season in 2016-2017 had more negative fluxes than the following two years, which was associated with a higher GCC from switchgrass remnants and winter weeds (Figures: 3.3, 3.2).

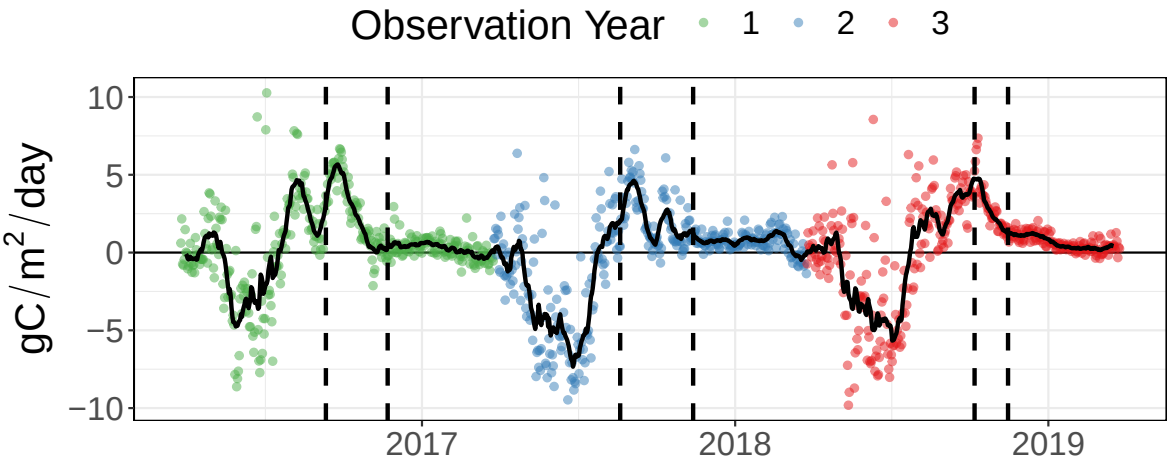

Figure 3.3: Daily sum of Net Ecosystem Exchange (NEE) for 2016 - 2019 at US-SB2. Colors indicate observation year used in the cumulative totals. The black trend line is a 14-day moving average. Dashed vertical lines indicate when the field was mowed (first line within a calendar year) and when the field becomes dormant (second line within a calendar year). Negative values indicate carbon being absorbed from the atmosphere

In the second observation year, emergence occurred on March 21, 2017, following a mild winter (Table: 3.2). NEE was negative for the first time on April 29, 2017, and did not become a source to the atmosphere until July 24th, 2017 (Figure 3.3). The daily uptake of carbon was higher in 2017 than in 2016, reaching -9.5 g C m^{-2} day^{-1} on June 20th, 2017 (Figure 3.3). The switchgrass was not completely brown before harvest occurred August 20, 2017, immediately followed by bailing and removal on August 23, 2017 (Figure 3.2, Table 3.1). This relatively early and quick harvest and removal allowed for significant secondary switchgrass growth and carbon uptake (Figure 3.2). Daily NEE totals remained

positive during the secondary growth, but the magnitude of CO_2 release was greatly reduced. Dormancy began on November 13, 2017. Some days with negative fluxes occurred during the 2017-2018 dormant season, but the site was predominately a minor carbon source during this period (Figure 3.3).

In the third observation year, emergence occurred on April 23, 2018, and NEE became negative for the first time on May 5, 2018 (Figure 3.3). Carbon uptake peaked at -9.82 gC m^{-2} day^{-1} on May 13th, 2018. The field remained a sink of carbon until July 24, 2018. Mowing did not occur until October 7, 2018, with bailing and removal a few weeks later, on October 24, 2018 (Table: 3.1). There was no evidence of secondary growth in 2018 in either the NEE or GCC. Any secondary growth that may have been underneath the brown upper switchgrass canopy would have been mowed on October 7th. During the dormant season, beginning on November 15th, daily NEE fluxes remained above 1 g C m^{-2} day^{-1} until Dec 27, 2018, after which fluxes reduced to near zero for the remainder of the study period. (Figure 3.3).

Diurnal NEE

Nighttime fluxes were largely similar between years, while large inter-annual differences were observed during the daytime. In April, daytime fluxes were more negative in year two than years one and three due to the early emergence (Figure 3.4, Table: 3.1). In May, June, and July, year one had slightly lower uptake rates than the following two years, -17 vs. -22.4 and -23.1 μmol m^{-2} s^{-1} in May, for example (Figure 3.4). In August, September, October, and November, the mean diurnal course of NEE was subject to the harvest and removal timing discussed above. In October, the rate of carbon uptake in year two was significantly higher than years one and three, related to the large secondary growth and the early harvest

that year (Figures: 3.4,3.2). The dormant season fluxes, December, January, February, and March, were small compared to other months. In January and February, year one had small but significantly higher carbon uptake rates and higher levels of GCC (Figures 3.4, 3.3). This maintenance of uptake over the winter in year one was a likely cause of the earlier and higher uptake rates in April of year two.

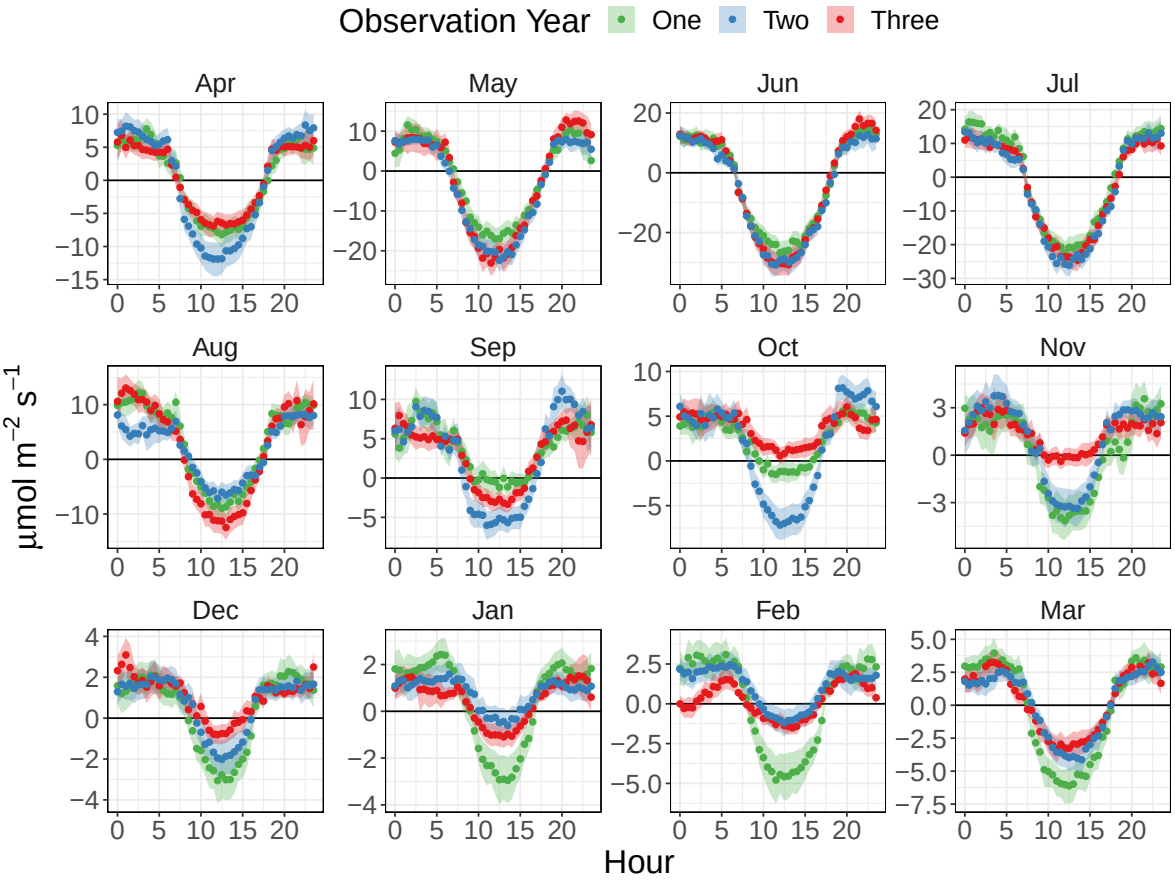

Figure 3.4: Mean hourly Net Ecosystem Ecosystem (NEE) for each month of each observation year at US-SB2. Shaded ribbon indicates the 95% confidence interval.

Cumulative Sums

Over the three observation years, this switchgrass field was a net carbon source to the atmosphere, releasing 239 (95% confidence interval: 193, 290) g C m^{-2} yr^{-1} (Table: 3.3). The site was a carbon source to the atmosphere during the first observation year (age 3), with a cumulative carbon release of 201 (171, 228) g C m^{-2} yr^{-1}. The second-year (age 4) was a small sink of carbon (-74 (-100, -47) g C m^{-2} yr^{-1}). The third-year (age 5) returned to being a carbon source to the atmosphere, with a cumulative carbon release of 112 (82, 144) g C m^{-2} yr^{-1}.

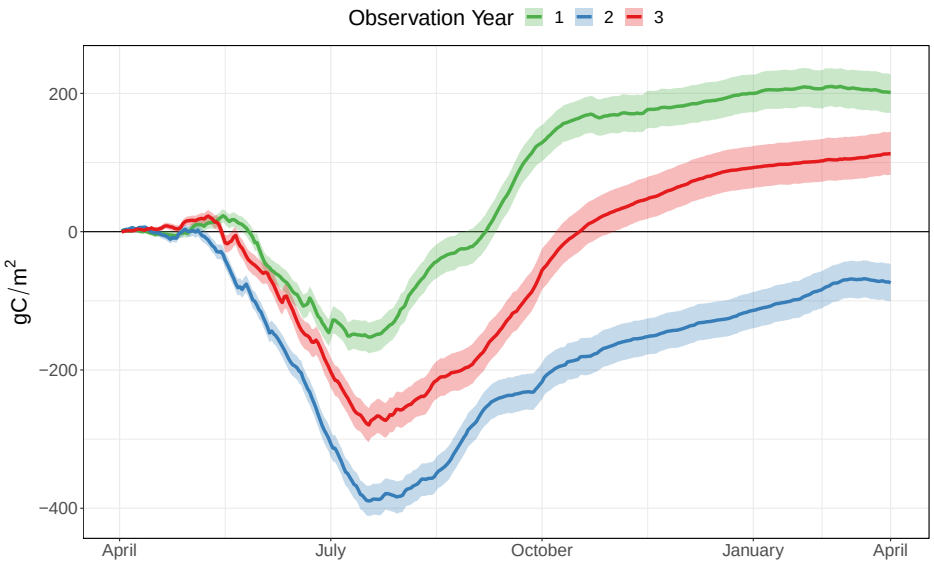

Figure 3.5: Cumulative sum of Net Ecosystem Exchange (NEE) over each observational year. Colors indicate observational year. Shaded ribbon indicates the 95% confidence interval of the cumulative sum since the beginning of the corresponding observation year. The observational year begins on March 26 each year.

Cumulative NEE over the growing season differed among the three years, while cumulative NEE during the non-growing season was similar. Interestingly, cumulative NEE reached its minimum on the same day each year (July 21) at, -153, -389, and -280 g C m^{-2} in years one, two, and three, respectively (Figure 3.5). Cumulative NEE at the end of the

growing season, defined as the harvest date, was -16.1, -357, and -87.6 g C m^{-2} (Table: 3.3). In the post-harvest season, the field released 186, and 191 g C m^{-2} in years one and two over 61 and 85 days. The post-harvest period in year three was only 39 days in length and released 117 g C m^{-2}. In the dormant seasons, the field released 33.3, 91.6 and 83.6 g C m^{-2} in years one, two, and three (Table: 3.3).

Table 3.3: Carbon budget of the US-SB2 switchgrass field (g C m^{-2})

	NEE						
Year	Growing	Post Harvest	Dormant	Total	Removed	NECB	Peak
2016-17	-16	184	33	201	126	327	362
2017-18	-357	191	92	-74	294	220	306
2017-19	-88	117	84	113	256	369	416
Total	-461	492	209	240	676	916	1084

At the annual time scale, cumulative RE and GPP were large. The field respired a total of 2195, 2604, and 2413 g C m^{-2} in years one, two, and three (Table: 3.4). Annual GPP fluxes were, 1994, 2680, 2273 g C m^{-2} in years one, two and three (Table: 3.4). As reflected in annual NEE fluxes, gross photosynthesis only exceeded respiration in year 2.

During the growing season, GPP exceeded RE. Respiration fluxes totaled 1651 and 1549 g C m^{-2} in years one and two, but was higher in year three with 2072 g C m^{-2} released during the growing season. GPP during the growing seasons were 1906 and 2160 g C m^{-2} in years two and three but lower in year one with 1667 g C m^{-2} absorbed (Table:3.4). Averaged across the three years, 82.5% of the gross photosynthesis and 73.1% of the respiration fluxes occurred during the primary growing season.

Nearly 20% of both GPP and RE fluxes occurred outside of the growing season. In the post-harvest season, GPP totals were small in years one and three (Table: 3.4). In year two, there was a significant amount of GPP in the dormant season, totaling 497 g C

m^{-2}. This is evident in the GPP, NEE, and GCC index (Figures 3.2, 3.3). RE was also elevated in year two in the post-harvest period with 687 g C m^{-2} released (Table: 3.4). In the dormant season, year one had the largest cumulative GPP (292 g C m^{-2}), despite a shorter dormant season duration (124 days) than the other years. Year three had low GPP during the dormant season, with only 92 g C m^{-2} absorbed (Table: 3.4). Dormant season RE in year three was also reduced with only 200 g C m^{-2} released, compared to greater than 300 g C m^{-2} released in years one and two (Table: 3.4).

Harvested biomass, reported by the operating company, ranged from 34% to 96% of peak above-ground biomass, as measured using clipped plots. Peak biomass carbon was 362, 306, and 416 g C m^{-2} in years one, two, and three, respectively (Table: 3.3). In contrast, harvested carbon was 126, 294, and 256 g C m^{-2}) in years one, two, and three (Table: 3.3). Only 34% of peak biomass of carbon was converted to harvested carbon in the first year of

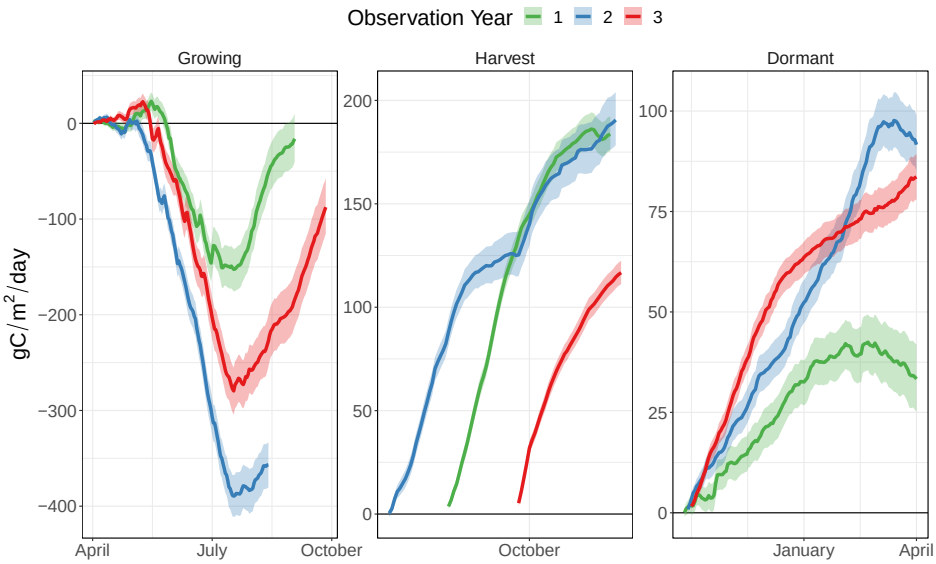

Figure 3.6: Cumulative sum of Net Ecosystem Ecosystem (NEE) at US-SB2 over the three major phases, growing season, post-harvest, and dormant. Colors indicate observational year. Shaded ribbon indicates the 95% confidence interval at each point in time.

observation. The low conversion was associated with the longest period between cutting and baling (Table: 3.1) and a corresponding large measured loss of carbon through atmospheric exchange in the post-harvest season (Table:3.5). The highest conversion (96%) was in year 2 when removal occurred only three days after cutting.

The Net Ecosystem Carbon Balance (NECB) is the sum of all incoming and outgoing carbon fluxes at the plot or field level (Chapin III et al., 2011). To calculate NECB at this site, we added the harvested carbon to the cumulative NEE sums for each observation year where the harvested carbon originated and ignored any other potential fluxes that are normally very small and not measured (e.g. dissolved organic carbon to groundwater, or biogenic volatile organic carbon to the atmosphere). This revealed that all years carbon sources, with years one, two, and three releasing 327, 220, and 269 g C m^{-2} yr^{-1}) to the atmosphere, respectively (Table: 3.3). Overall, NECB showed less inter-annual variability than NEE (NECB sd: 53 g C m^{-2} yr^{-1}; NEE sd: 140 g C m^{-2} yr^{-1}) .

Table 3.4: Gross Ecosystem Production (GPP) and Ecosystem Respiration (RE) of the US-SB2 switchgrass field (g C m^{-2} yr^{-1})

Year	Growing	Post Harvest	Dormant	Total
		GPP		
2016-17	1667	35	292	1994
2017-18	1906	497	277	2680
2017-19	2160	20	92	2272
Total	5733	552	661	6946
		RE		
2016-17	1651	219	325	2195
2017-18	1549	687	368	2604
2018-19	2072	137	203	2412
Total	5272	1043	896	7211

3.5 Discussion

We found that an operational switchgrass field in central Virginia was a carbon source to the atmosphere when integrated over the three observation years. This differs from NEE reported at other switchgrass EC studies, where most sites were net sinks of carbon from the atmosphere over their observation periods (Figure 3.7). Our site differs from the other sites in multiple ways, including the combination of climate conditions, management activities, and land-use history.

Previous EC switchgrass studies included annual nutrient fertilization after establishment, while our site had no nutrient fertilization application after planting. The effect of fertilization on the net source or sink status of a switchgrass field is uncertain. While nitrogen additions have been shown to increase above-ground biomass, they can also reduce allocation to below-ground biomass and increase root litter and soil decomposition (Stewart et al., 2016). This would suggest that our unfertilized field could have reduced below-ground respiration. However, the lack of nitrogen additions increases the likelihood that this field is nitrogen limited. Grass species have been shown to prime soil decomposition through root exudation, presumably in search of nutrients, thus increasing respiratory losses (Shahzad et al., 2015).

For our switchgrass field to be a carbon source to the atmosphere over the three observations years at ages 3-5 since field establishment, the field must be releasing carbon that accumulated in the ecosystem during the prior land-use or the first 2 years of switchgrass growth. Before conversion to switchgrass, the field was a perennial C3 grassland used for hay production. Other studies examining post-conversion carbon balance have found carbon losses when the previous land-use was natural grassland with large soil carbon stocks (Abraha et al., 2018). This field may continue to respire this legacy carbon even after 5 years under

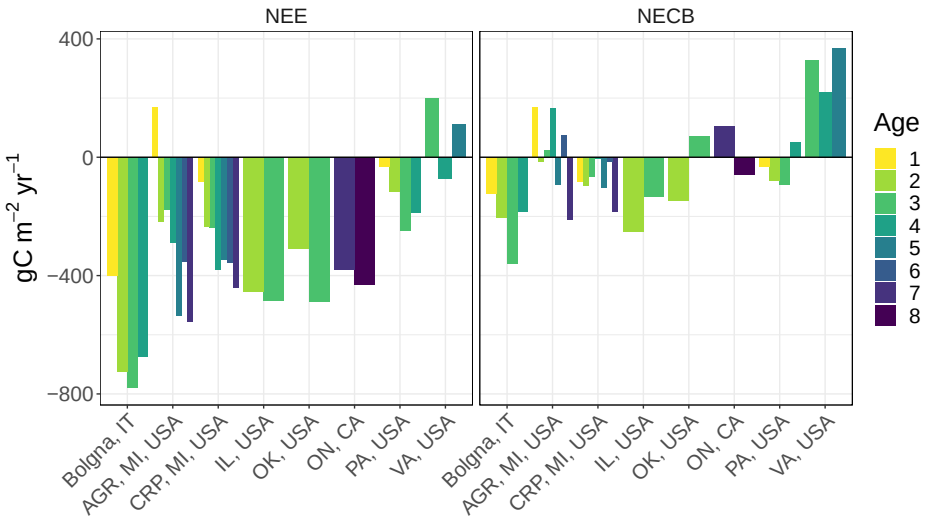

Figure 3.7: Overview of annual carbon balance, with and without accounting for harvested carbon, for published eddy covariance switchgrass studies and this study, (Abraha et al., 2018, Di Virgilio et al., 2018, Eichelmann et al., 2016a, Skinner and Adler, 2010, Wagle and Kakani, 2014, Zeri et al., 2011)

the new land-use. Future work at our site will use carbon isotopes to detect differences in soil respiration between C3 and C4 carbon.

While our switchgrass field was a carbon source annually, fluxes during the growing season were similar to other studies. Wagle and Kakani (2014) only measured fluxes during the growing season; their averaged 1603 g C m^{-2} yr^{-1} of GPP and 1205 g C m^{-2} yr^{-1} of RE (Table: 3.5). Our site measured 1911 g C m^{-2} yr^{-1} of GPP on average during the growing season, and 1757 g C m^{-2} yr^{-1} of RE. In addition, the magnitude of the daily fluxes of our field is very similar to other studies. For example, our average peak daily uptake was -9.3 gC m^{-2} day^{-1}, which is similar to Eichelmann et al. (2016a) with approximately -11.7 gC m^{-2} day^{-1}, and Wagle and Kakani in 2012 with -9.8 gC m^{-2} day^{-1}. Furthermore, our diurnal fluxes are also comparable with other studies. However, while other studies observe non-growing season fluxes that are slightly positive or near zero (Eichelmann et al., 2016a, Skinner and Adler, 2010, Wagle and Kakani, 2014), we measured consistently positive fluxes

as early as July 18th, leading to substantial losses of carbon as high as 10.3 gC m^{-2} day^{-1} (Figures:3.3,3.6. This carbon source is then enhanced or maintained by harvest activity in the late summer.

While the cumulative sum of NEE over the three years was positive, NEE showed inter-annual variability with, one of the three years exhibiting negative NEE. However, this inter-annual variability was not as substantial in the NECB estimates that combined NEE and harvested carbon (Table 3.3) because the years with lower NEE had higher baled yields. In contrast, peak biomass, measured as senescence begins, had low variation inter-annually (Table: 3.3). The higher inter-annual variability for the baled yield than peak biomass suggests that the timing of fall harvest has a substantial impact on cumulative NEE. If the harvest is late, the carbon is released in the field as fugitive losses (Sanderson et al., 1996). This is especially noticeable in 2016 when the cutting and baling are separated in time by over a month, leading to large positive fluxes of carbon during that period (Figure 3.6). If the harvest is early and removed from the field quickly, fugitive losses are reduced as in 2017 (Table: 3.3). Only when that removed carbon is added back into the carbon balance estimate as assumed emissions, as occurs when used for bioenergy, that we see the field was a net carbon source to the atmosphere.

This work has implications for both national bioenergy policy and field-scale management decisions. Previous work has suggested that biofuel crops benefit climate by offsetting CO_2 and increase below-ground carbon storage (Adler et al., 2007, Anderson-Teixeira et al., 2013). However, there can be large differences in carbon sequestration rates based on species, region, age, and land-use history (Abraha et al., 2018, Di Virgilio et al., 2018, Eichelmann et al., 2016a, Follett et al., 2012, Zeri et al., 2011). At this relatively warm and humid switchgrass site that was converted from an old pasture, we found no net carbon sequestration three to five years after switchgrass establishment. This differs from previous

work that has shown switchgrass fields to be a carbon sink or, only a small carbon source even when harvested carbon is added to the annual sums. In terms of management, this study showed that delaying harvest or allowing cut grass to lay for an extended period substantially increased net carbon losses to the atmosphere. This study illustrates that predictions of net carbon climate benefits from bioenergy crops can not assume that the ecosystem will be a net sink of carbon from the atmosphere. Climate, management, and land-use history may determine whether the widespread deployment of switchgrass as a bioenergy feedstock results in realized climate change mitigation. Future analyses need to consider this variation when assessing the climate benefits of switchgrass and other bioenergy crops.

Table 3.5: Annual carbon balance, climate, and fertilization rate from published eddy covariance switchgrass studies and this study

Age	Year	GPP	RE	NEE	C Removed	NECB	Precipitation	Temperature	N Rate
Years		g C m^{-2}	g C m^{-2}	g C m^{-2}	g C m^{-2}	g C m^{-2}	mm	°C	kg N ha^{-1}
Virginia, USA									This Study
3	2016 -17	-1994	2195	201	126	327	1080	15.0	0
4	2017 -18	-2680	2604	-74	294	220	835	13.9	0
5	2018 -19	-2272	2412	113	256	369	1668	15.6	0
Ontario, CA									Eichelmann et al. (2016a)
7	2012	-1354	833	-380	486	106	533	9.4	78
8	2013	-1430	869	-430	371	-59	868	7.2	101
Pennsylvania, USA									Skinner and Adler (2010)
1	2004 -05	-941	911	-31	0	-31	868	10.0	0
2	2005 -06	-916	798	-118	38	-80	995	9.7	56
3	2006 -07	-926	678	-248	154	-94	1071	9.9	56
4	2007 -08	-915	726	-189	239	50	1059	9.8	56
Oklahoma, USA									Wagle and Kakani (2014) *
2	2011	-1192	884	-308	160	-148	525	16.7	75
3	2012	-2015	1526	-490	560	70	673	17.2	76
Illinois, USA									Zeri et al. (2011)
2	2009			-453	200	-253	1302	10.6	0
3	2010			-485	350	-135	931	11.7	56
Bolgna, Italy									Di Virgilio et al. (2018)
1	2012 -13	-1191	786	-402	280	-122	575	14.4	0
2	2013 -14	-1666	937	-726	520	-206	802	13.9	50
3	2014 -15	-1755	5	-780	420	-360	829	15.0	50
4	2015 -16	-1544	870	-675	490	-185	679	14.4	50
Michigan, USA (AGR)									Abraha et al. (2018)
1	2010			170	0	170	936	10.0	0
2	2011			-217	201	-16	975	9.0	56
3	2012			-177	201	24	796	11.3	56
4	2013			-289	453	164	1139	9.1	56
5	2014			-535	441	-94	971	7.5	0
6	2015			-355	430	75	1173	8.4	56
7	2016			-555	345	-210	948	10.7	56
Michigan, USA (CRP)									Abraha et al. (2018)
1	2010			-82	0	-82	936	10.0	0
2	2011			-235	138	-97	975	9.0	56
3	2012			-237	171	-67	796	11.3	56
4	2013			-382	376	-6	1139	9.1	56
5	2014			-346	244	-102	971	7.5	0
6	2015			-357	342	-15	1173	8.4	56
7	2016			-442	259	-183	948	10.7	56

* Cumulative sums from the growing season only

Chapter 4

Land-cover decisions result in global radiative forcing trade-offs: comparing the establishment of a pine plantation to a bioenergy cropland for climate mitigation

4.1 Abstract

The restoration and expansion of forested lands has led to a decrease in atmospheric carbon dioxide and is a natural solution for climate change mitigation. However, forests also have relatively low albedo compared to grass and croplands, which increases the energy absorbed at the surface. An alternative natural climate solution is to replace fossil fuel usage with bioenergy. Bioenergy crops such as switchgrass have higher albedo than forest ecosystems but absorb less total carbon over their lifetime. To evaluate trade-offs in the mitigation potential by pine and switchgrass ecosystem, we used eddy covariance data collected from planted pine forests and switchgrass fields in eastern North America to assess how a decision to replace a perennial bioenergy crop with a planted pine forest alters net radiative forcing. We found the combined radiative forcing from albedo and carbon results in pine having a warming influence with a net positive radiative forcing of 9.8 $Wm^{-}2$ (30 year mean). However, eddy covariance towers do not measure carbon removed from the ecosystem through harvesting. When we assumed all harvested bioenergy crop carbon was emitted to the atmosphere and that the harvested pine forest carbon was prevented from entering the atmosphere, the 30-year mean net radiative forcing was near zero (0.35 $Wm^{-}2$). Therefore the climate service of forests absorbing carbon dioxide is offset by the reduction of albedo, making perennial bioenergy crops a viable alternative natural climate solution.

4.2 Introduction

The establishment and protection of forests is a potential natural climate solution (NCS) by mitigating anthropogenic climate change through the maintenance of carbon stored in forest biomass and the removal of CO_2 from the atmosphere through growth (Bastin et al., 2019, Hemes et al., 2021, Pacala, 2004). However, forests have a lower albedo than alternative land-cover types, such as agriculture or grasslands, which increases the amount of radiation absorbed at the surface (Jackson et al., 2008). Depending on the location, the decrease in albedo associated with a forested land-cover can offset the climate benefit provided by sequestered carbon (Bala et al., 2007, Betts, 2000, Bonan, 2008a). This is especially pronounced at high latitudes where there is a large discrepancy in albedo between a tall, dark forest and a short crop or grassland covered by snow from the late fall through early spring. In temperate latitudes, the albedo difference is less pronounced because snow cover is less frequent(Betts, 2000). As a result, the albedo influence on the radiative energy balance can be similar to the carbon influence(O'Halloran et al., 2012). Therefore, to determine the climate benefits of a land-cover and land-management decisions in the temperate region, it is critical to quantify the combined impact of the change in carbon and albedo on global climate.

An alternative NCS to forest establishment for carbon absorption and storage is the replacement of fossil fuel energy sources with a dedicated bioenergy crop. The above-ground biomass of a bioenergy crop is burned shortly after harvesting for energy and below-ground biomass increases carbon accumulated in the soil, resulting in the net removal of CO_2 from the atmosphere (Anderson-Teixeira and DeLucia, 2011). Crops and grasses, including perennial bioenergy crops such as *Miscanthus* and switchgrass, also have higher albedo values than forests (Bonan, 2008a, Miller et al., 2015). The direct effect of the higher albedo of perennial bioenergy crops on atmospheric radiation balance can be large. One study found it to be

six times larger than the offset of fossil fuel use (Georgescu et al., 2011). Therefore it is unknown how a decision to establish a forest with high production and potential for long-term carbon storage in wood compared with the higher albedo from a bioenergy crop affects the land-cover decision's net climate benefits.

Changes in albedo and carbon dioxide influence the planetary energy balance and global temperatures, but through different mechanisms. A change in surface albedo directly affects the amount of sunlight absorbed and reflected at the surface (Bonan, 2008a). A change in atmospheric carbon dioxide affects the absorption of emitted long-wave radiation by the atmosphere, reducing the energy emitted by the top of the atmosphere. The different pathways and time dependencies of these effects requires modeling to translate the units of radiation associated with albedo to carbon units or vice versa. Here we use the radiative forcing metric (Hansen et al., 1997), which converts a change in carbon stocks into a change in carbon dioxide concentrations and then converts this to a change in planetary energy balance. To calculate a radiative forcing, it is important to capture the net carbon fluxes of the ecosystem with respect to the atmosphere. Measurements of above-ground biomass and even carbon stocks in general potentially miss fluxes of carbon out of the ecosystem potentially overestimating carbon storage. In combination with the need for accurate albedo measurements, eddy-covariance (EC) towers are ideally suited to make these calculations. EC towers typically measure the net flux of carbon and water into and out of the atmosphere (Aubinet et al., 2012). A typical EC tower includes measurements of incoming and outgoing shortwave radiation required for calculating albedo.

We compare the influence of managed pine stands to managed bioenergy crop fields on global climate using observations of carbon storage and albedo. We focus on comparing a pine plantation with a switchgrass field because they are managed ecosystems that use species with overlapping ranges. In the Southeastern United States (SEUS), pine plantations are

most commonly planted with loblolly pine, a wide-spread fast-growing native species that can be used for timber or bioenergy (Wear and Greis, 2013). A typical rotation length for a pine plantation is between 15 and 30 years (Fox et al., 2007, Stanturf et al., 2003, Wear and Greis, 2013). Switchgrass is a native, C4, perennial grass species that has emerged as a promising bioenergy feedstock with high expected yields for the SEUS (McLaughlin and Adams Kszos, 2005, Parrish and Fike, 2005, Wullschleger et al., 2010). Both species are reported to do well on marginal lands and can even be inter-cropped (Albaugh et al., 2014). Unlike a pine plantation that is harvested at the end of the rotation with possible thinning at intermediate ages, switchgrass is harvested each year. Therefore, including the entire cycle of establishment and harvest for both systems is critical for a robust comparison of radiative forcing.

Here we ask, 1) over a typical rotation, which ecosystem (pine plantation vs. bioenergy crop) results in the lowest radiative forcing and; 2) how do assumptions about the fate of harvested carbon influence the conclusions? To address these questions, our study combines published data from eddy covariance sites in the Eastern U.S. and Canada that are in pine plantations and switchgrass fields with new observations from an eddy covariance study in Virginia that includes a pine plantation, switchgrass field, and a recent clear-cut. Together these studies provide data used to model the relationship between age since establishment,net ecosystem productivity, and albedo. The age vs. albedo and net ecosystem production (NEP) relationship is used with an established method for calculating relative forcing over a 30-year time horizon that includes one complete harvest rotation of a pine plantation and annual harvests of switchgrass.

4.3 Methods and Materials

We describe our new eddy-covariance site and data processing, the synthesis of existing eddy-covariance sites, the development of the NEP and albedo curves over a full rotation for both the pine plantation and switchgrass fields, and the modeling of radiative forcing.

4.3.1 New eddy-covariance measurements

Site Description

This study uses data collected from three co-located eddy covariance towers located in central Virginia. The climate of this region is humid subtropical (Köppen climate classification Cfa), with warm humid summers and cool mild winters. The first tower (Ameriflux designation: US-SB1, Pine hereafter) was over a mixed age loblolly pine plantation and began measurements May 6th, 2015. The second tower (US-SB2, Grass hereafter) is over a Switchgrass field that was harvested annually for bioenergy and began measurements March 26th, 2016. The third tower (US-SB3, Clearcut hereafter) was over a clear-cut loblolly pine stand that was harvested and removed in late 2017; measurements began March 28th, 2018. These three towers were within 1.6 km of each other, ensuring that each system share weather conditions and soil characteristics.

Measurement of Carbon and Albedo

Each site was equipped to measure meteorological data and an eddy covariance system to measure carbon dioxide and water fluxes. Each tower measured incoming and outgoing shortwave radiation with a CNR4 four-way net radiometer (Model CNR4, Kipp and Zonen). Albedo (α) was calculated from the ratio of mid-day incoming (S_i) and outgoing (S_o) short-

wave radiation ($\alpha = S_o/S_i$). The CNR4 of the pine tower was 26 meters above ground level, 4 - 6 meters above the upper canopy (20 - 22 meters in height). At the clearcut and grass towers, instruments were mounted on a tripod tower, with the CNR4 at a height of 4 meters and extended away from the tower base to avoid non-vegetation in the instruments view shed. Meteorological measurements were logged on a data logger (Model XLite 9210, Sutron).

Each tower was equipped with an eddy covariance (EC) system that was used to measure the flux of carbon dioxide. Gas concentrations were measured with a closed-path infrared gas analyzer (LI-7200, Licor) at the pine and grass towers at 26 and 4 meters, respectively. The clearcut tower was equipped with an open-path infrared gas analyzer (LI-7500, Licor) 4 meters above ground level. Each tower had a 3D sonic anemometer (WindMaster, Gill Instruments) co-located with the gas analyzer based on manufacturer recommendations. Data were collected continuously at 10 Hz and averaged to 30 minute time intervals using EddyPro version 6.2.2 (LI-COR, Inc., 2019). We implemented a double-rotation method to account for tilt in the anemometer, a block average detrending method, and compensation for density fluctuations. Quality checks were performed according to (Foken et al., 2004). Raw data were screened for spikes, amplitude resolution, drop-outs, absolute limits, skewness, and kurtosis (Vickers and Mahrt, 1997). Footprint estimation was performed according to (Kljun et al., 2004). Because this footprint model is dependent on canopy height, we supplied a dynamic height file to the EddyPro software that describes the rapidly changing height of the switchgrass. Height was determined by visually inspecting PhenoCam images (Seyednasrollah et al., 2019), using a vertical PVC pipe in the field, marked every 10cm from the ground up to two meters. We did not include an angle of attack correction, as the available correction includes an artificial inflation of the vertical wind measurement (LI-COR, Inc., 2019). The anemometer at the pine tower is subject

to the w-boost issue, and corrections were applied to offset the bias according to LICOR recommendations.

We applied a friction velocity filtering routine to remove data with inadequate turbulence. We determined the friction velocity threshold by examining the relationship between friction velocity and net ecosystem exchange (NEE) fluxes as in Papale et al. (2006) using the REddyProc R-package (version 1.2) (Wutzler et al., 2018) for all three towers independently and filtered out data that fell below this threshold.

In order to obtain annual and seasonal totals of NEE, we filled the gaps resulting from measurement interruptions or filtering with modeled values using the REddyProc R-package (version 1.2) marginal distribution sampling algorithm (Reichstein et al., 2005, Wutzler et al., 2018), a widely-used approach. This method utilizes the co-variation of fluxes with meteorological variables and the temporal auto-correlation with time of day. Gaps are filled by applying averages derived for a specific time of day, time of year, and meteorology. We converted NEE to NEP where NEP = -NEE.

4.3.2 Modeling Carbon and Albedo

To create a time series of albedo and NEP for both ecosystem types we combined Virginia site observations with published and publicly available EC data of pine and switchgrass ecosystems. Annual NEP values for pine stand were gathered from this study,Bracho et al. (2018), and Bracho et al. (2012). Annual NEP values for switchgrass were obtained from these studies, Abraha et al. (2016), Eichelmann et al. (2016a), Skinner and Adler (2010), Zeri et al. (2011). Annual albedo values for pine were obtained from this study and publicly available data on the Ameriflux repository from Noormets (2016, 2018), Oishi et al. (2016). Albedo values for grass were obtained from this study only. We determined the age of the

annual albedo and NEP values from reported ages where given, and from taking the difference between reported year of observation and year of establishment. Overall, we developed a age-based time-series for albedo and NEP in both pine and switchgrass ecosystems. The time series was used to fit models that described NEP and albedo as a function of age.

First, we modeled NEP of both systems with a three parameter Michelis-Menton equation that included an intercept.

$$y = c + (d - c) \times \left(\frac{x}{x + e} \right) + \epsilon \tag{4.1}$$

where y is the NEP of the ecosystem, x is the age, c is the y intercept, d is the saturation value, and e is the age at half saturation. Secondly, albedo was modeled as a constant for the switchgrass ecosystem,

$$y = c + \epsilon \tag{4.2}$$

and with a three parameter asymptotic relationship for loblolly pine.

$$y = a + (b - a) \times (1 - e^{-x/c}) + \epsilon \tag{4.3}$$

For all models ϵ is normally distributed random error with a mean of zero and standard deviation of σ

All four models were fit using a Bayesian framework with non-informative priors. The rjags package (Plummer, 2019) was used to generate the joint posterior distributions of the parameters. We ran three chains for 10,000 iterations with a 1,000 iterative burn-in and evaluated convergence using the Gelman, Rubin, and Brooks convergence diagnostic

(Gelman et al., 1992). To generate posterior predictions, we generated 5000 samples from the joint posterior distribution of the parameters, calculated the NEP and albedo at each age using each sample, and added randomly distributed noise based using the σ parameter associated with each model. However, radiative forcing from an albedo change is ideally calculated monthly (Bright et al., 2015). To generate monthly predictions of albedo, we calculated the average observed bias of each month from the annual mean and applied this bias to the annual predictions described above. Each set of 5000-sample time series for NEP and albedo was used to calculate the 95% predictive intervals and used in the radiative forcing calculations described below.

4.3.3 Radiative Forcing

Albedo

Albedo (α) is calculated as the ratio of mid-day (11:00 - 13:00) outgoing (S_o) and incoming (S_i) shortwave radiation and aggregated to the monthly time step.

$$\alpha = \frac{S_o}{S_i} \tag{4.4}$$

The change in albedo is calculated at the monthly scale:

$$\Delta\alpha(i, m) = \alpha_p(i, m) - \alpha_g(i, m) \tag{4.5}$$

where α_p is the albedo of the pine stand, and α_g is the albedo of the grass field, i is the year, and m is the month.

The annual radiative forcing from a change in albedo is calculated as:

$$\Delta F_{\alpha}(i) = \frac{\sum_{m=1}^{m=12} K(m)\Delta\alpha(i,m)}{12} \tag{4.6}$$

where $K(m)$ is the monthly $Wm^{-}2$ change in shortwave absorption resulting from a 100% change in albedo. We extracted $K(m)$for the Virginia site from a gridded global radiative kernel product (Bright and O'Halloran, 2019).

Carbon

The radiative forcing of a carbon change from one square meter of ground is calculated:

$$\Delta F_{c}(i) = 5.35 \times \ln\left(1 + \frac{\Delta C(i)/2}{400 \times 21.34^{14}}\right) \times 51^{13} \tag{4.7}$$

where $\Delta C(i)$ is the change in change in carbon balance between the pine and grass systems for year i, "21.34^{14}" is the weight in grams of 1 ppm of carbon calculated from first principles, "51^{13}" is the surface area of the earth, 400 ppm is used as a baseline carbon dioxide concentration, "5.35" ($Wm^{-}2$) is conversion factor that converts from carbon dioxide ppm units to radiative forcing (Betts, 2000, Kirschbaum et al., 2011, O'Halloran et al., 2012). The factor of 2 roughly addresses the amount of released carbon that remains in the atmosphere annually (Cavallaro et al., 2018).

We used four scenarios to test the sensitivity of our findings to assumptions about the fate of harvested carbon. Scenario A assumes that none of the harvested carbon from either ecosystem is emitted to the atmosphere. Scenario B assumes that all of the harvested pine carbon is emitted to the atmosphere, but none of the harvested switchgrass carbon is emitted. Scenario C assumes that all of the harvested switchgrass carbon is emitted to the

atmosphere, but none of the harvested pine carbon is emitted. Scenario D assumes that all of the harvested carbon from both ecosystems is emitted to the atmosphere. While it is unlikely that all or none of the harvested carbon is emitted atmosphere in practice, these scenarios examine the sensitivity by evaluating the end members of possible outcomes.

The scenarios requires estimates for harvested carbon from each ecosystem. Yields for both pine and switchgrass are highly variable in time and space (Fox et al., 2007, Parrish and Fike, 2005, Wear and Greis, 2013). Therefore we used average expected yields for both ecosystems from literature values. For switchgrass, we used an average reported yield of 8.7 $Mg/ha/yr$ (Wullschleger et al., 2010), assumed a carbon content of 42% (Eichelmann et al., 2016a), which converts to 365.4 $gC/m^2/yr$. We applied this harvest value to each non-establishment year of our simulated switchgrass field (excludes year 1,11, and 21) resulting in 9,866 gC/m^2 total harvested carbon. In the pine ecosystem of we assumed dry yields of 4 $tons/acre/yr$ as reported in Stanturf et al. (2003), assumed a 50% carbon content (Chapin III et al., 2011), which converts to 448.3 $gC/m^2/yr$. This value was applied for each year of the simulated pine stand, except for the pre-establishment year (excludes year 1) 13,000 gC/m^2 total harvested carbon.

4.4 Results

Observed Albedo and NEP at new Virginia site

At our Virginia three-tower site, the mean annual NEP in the 27-30 year old loblolly pine plantation over the 4-years of measurements was 896 $gC\ m^{-2}\ yr^{-1}$ with a range of 659 to 1014 $gC\ m^{-2}\ yr^{-1}$ (Table 4.1). The mean annual NEP in the 3-5 year old Switchgrass field was 80 $gC\ m^{-2}\ yr^{-1}$ for the 3-years of measurement. The switchgrass included two years

with negative NEP, where the switchgrass field was a source of carbon to the atmosphere. The single year of measurement at the clearcut site (representing a 0 aged pine plantation) was a carbon source, releasing 658 $gC\,m^{-2}\,yr^{-1}$ to the atmosphere. (Table 4.1).

The pine plantation had lower albedo than both grass and clearcut. On average, the albedo at the pine (0.2) was 0.1 darker than the grass and clearcut (Table 4.1). The albedo at the pine plantation and switchgrass showed low inter-annual variability.

Table 4.1: Average annual net ecosystem productivity (NEP; $gC\,m^{-2}\,yr^{-1}$) and albedo (unit-less) for the pine, grass, and clearcut eddy covariance towers at Sweet Briar College.

	2015	2016	2017	2018
Loblolly Pine (US-SB1)				
Albedo	0.11	0.12	0.11	0.10
NEP	659	1014	915	995
Switchgrass (US-SB2)				
Albedo		0.21	0.20	0.21
NEP		-201	74	-113
Clearcut (US-SB3)				
Albedo				0.19
NEP				-658

4.4.1 Models of albedo and NEP through ecosystem development

Combining the annual NEP measurements from our Virginia pine plantation with published values revealed a clear saturating relationship with stand age. The pine plantations released carbon for the first 5 years before becoming carbon sink as the stand continues to mature to a typical rotation length of 30-years. The pine plantations initially released 1050 $gC\,m^{-2}\,yr^{-1}$(-1590, -517; 95% predictive interval) to the atmosphere. Productivity increased quickly and the pine plantation was neutral by year 4 (Figure 4.1). Productivity continued

to increase each year but the rate of increase slows over time. In year 30, pine NEP peaked at $903 gC\, m^{-2}\, yr^{-1}$(436, 1360; 95% predictive interval).

In contrast to the pine plantation, the modeled switchgrass field quickly became a net sink of CO_2 after establishment (Figure 4.1). One key outlier was the Virginia site where switchgrass was a source in multiple years following establishment (Chapter 3). As a result of including the Virginia site, the 95 % predictive intervals in the age vs. NEP relationship for switchgrass overlapped zero for the first six years following field establishment (Figure 4.1). Maximum NEP was $100 gC/m^2/yr$ lower than the pine plantation at peak productivity. While observed data did not extend beyond age 8 we extrapolated to age 10 so that three 10-year switchgrass rotations can be compared to one 30-year pine plantation rotation in the radiative forcing calculations

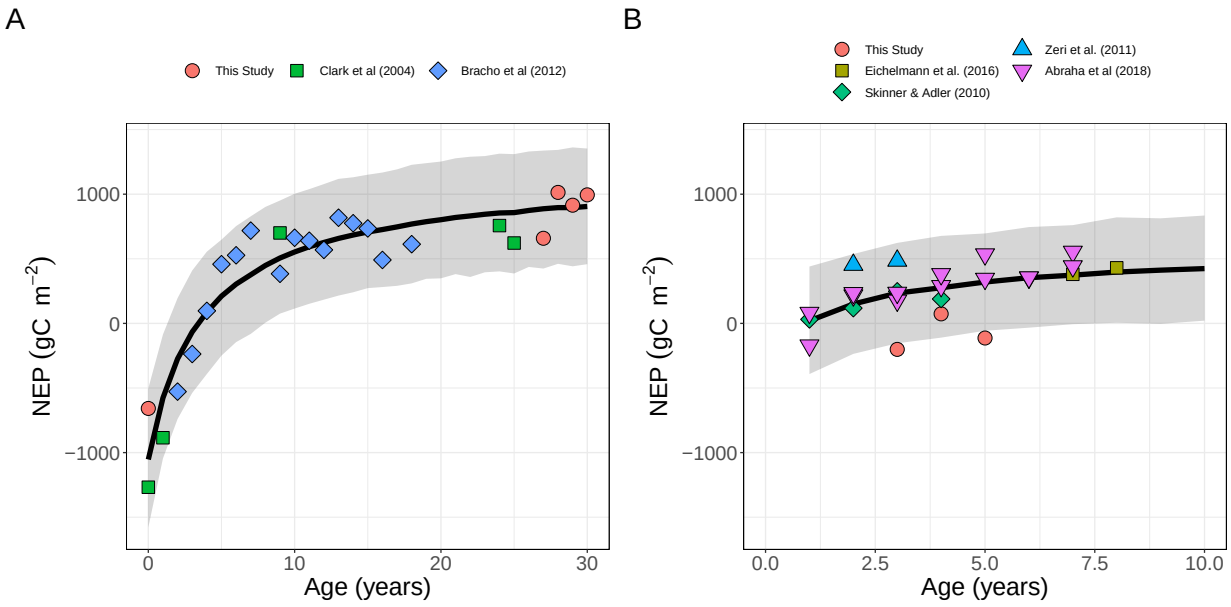

Figure 4.1: Annual net ecosystem production for a) Loblolly pine and b) Switchgrass over a 30-year and 10-year rotation, respectively. Points represent annual NEP reported from this study and published values using eddy-covariance measurements. The black line represents the mean for the modeled fit. The gray shaded region represent the 95% confidence interval. Data are from this study; Abraha et al. (2018), Bracho et al. (2012), Clark et al. (2004), Eichelmann et al. (2016a), Skinner and Adler (2010), Zeri et al. (2011).

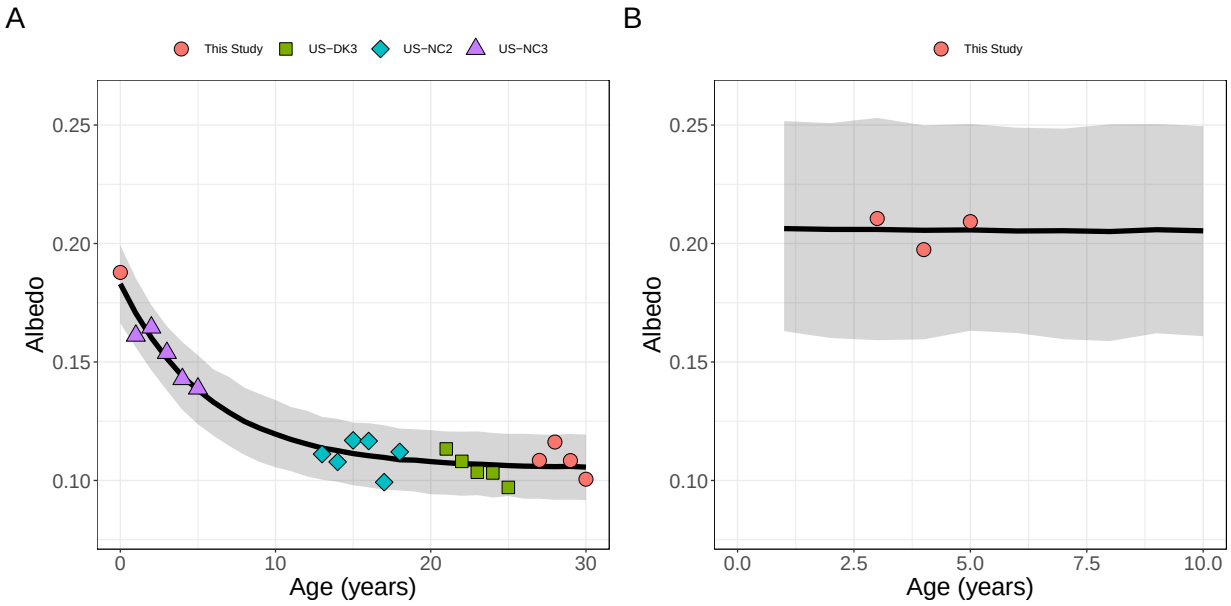

Figure 4.2: Albedo for a) Loblolly pine and b) Switchgrass over a 30-year and 10-year rotation, respectively. Points represent annual average albedo calculated from our site and publicly available data through Ameriflux. The black line represents the mean for the modeled fit. The gray shaded region represent the 95% confidence interval. Data are from this study; Noormets (2016, 2018), Oishi et al. (2016)

Similar to NEP in the pine plantation, albedo showed a clear saturating relationship with age. The age 0 stand (i.e., the year following the clear-cut) had an albedo of 0.18(0.17 - 0.19; 95% predictive interval) (Figure 4.2). As the canopy closed, albedo reduced quickly and reaching half the lowest value at year 3. By year 15, albedo was nearly constant through age at a value of 0.11(0.10 - 0.12; 95% predictive interval).

While we found limited switchgrass albedo data beyond our Virginia site, albedo at our Virginia site showed low variability over the three years of measurement. Furthermore, the albedo was similar to the clearcut site with limited vegetation, indicating that the albedo of a newly established switchgrass field with limited vegetation would likely have similar albedo to a more mature switchgrass field. Therefore, we modeled the switchgrass field as constant through age with a value of 0.21(0.16 - 0.25; 95% predictive interval). The wide

confidence intervals reflect the limited available data.

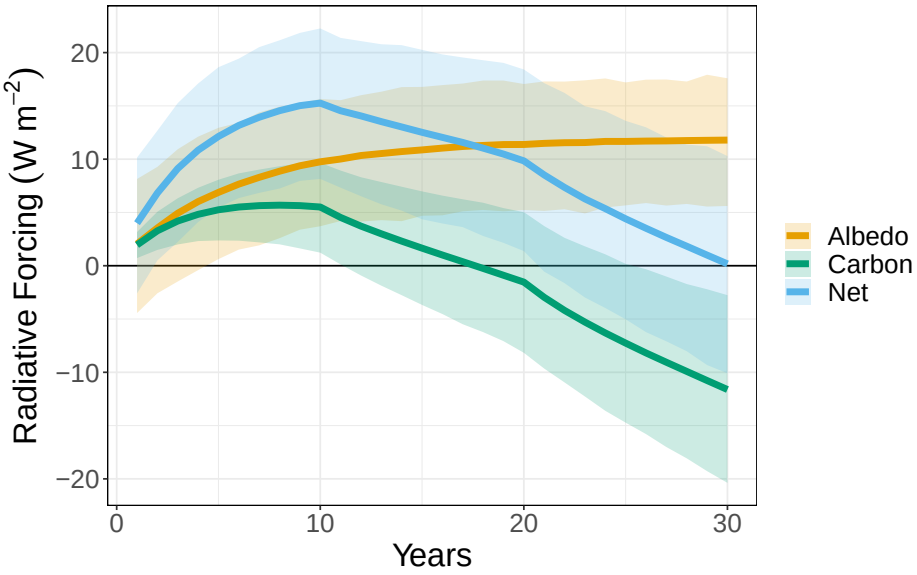

Figure 4.3: The radiative forcing due to a change in carbon balance, albedo, and the combination that results the decision to establish either a switchgrass field or loblolly pine stand. Positive values indicate that loblolly pine has a warming effect when compared to switchgrass while negative values indicate that pine has a cooling effect when compared to switchgrass.

4.4.2 Radiative Forcing

Using the modeled albedo and NEP, we calculated the annual radiative forcing that would occur if a pine plantation was established instead of a switchgrass field. Therefore, in our analysis, positive numbers indicate that the pine plantation increases energy at the top of the atmosphere, increasing the amount of energy available to warm the atmosphere. Due to the initial losses of carbon from pine plantation and the rapid growth of the switchgrass field, the radiative forcing from a change in carbon balance (ΔF_c) was positive for the first 17 years, peaking in year 8 at 5.7(2.0 - 9.3; 95% predictive interval) Wm^{-2} (Figure 4.3. The ΔF_c became negative in year 18 and continued to decline to -11.6(-20 - -2.7) Wm^{-2} at the end of the 30 year period.

The modeled pine plantation was darker than the modeled switchgrass at all ages. However, this difference was minimized in ages 0 through 10 as the higher albedo clearcut transitioned to a closed canopy forest (Figure 4.2). As a result, the radiative forcing from a change in albedo (ΔF_α) was always positive over the 30-year rotation. ΔF_α in the first year was 2.0(-4.4- 8.1; 95% predictive interval) Wm^{-2} with a maximum in year 30 at 11.8(5.6 - 17.6) Wm^{-2} (Figure 4.3).

The total radiative forcing (ΔF_{net}) over the whole 30 year period was positive (Figure 4.3). The ΔF_{net} in year one was 3.9(-2.6 - 10.1; 95% predictive interval) Wm^{-2}, and reached the maximum in year 10 at 15.3(8.1 - 22.3) Wm^{-2}. In year 30, ΔF_α and ΔF_c offset each other, resulting in ΔF_{net} centered at 0.17(-10 - 10) Wm^{-2}. Despite ΔF_α and ΔF_c offset each other at year 30, the average annual radiative forcing (ΔF_{net}) over the 30-year period was positive 9.8(6.5 - 12.8; 95% predictive interval) Wm^{-2}, indicating that negative forcing from NEP in the mature pine stand was not large enough to compensate for the loss of carbon at younger ages and the lower albedo Figure 4.4.

We examined the sensitivity of ΔF_c and ΔF_{net} to assumptions about the fate of the harvested carbon by assuming two extremes - either all harvested carbon (using literature derived estimates as described in the methods) returns to the atmosphere during the 30-year analysis period or none of the harvested carbon returns to the atmosphere. Scenario A is reported above, where no harvested carbon returns to the atmosphere for either ecosystem. The average ΔF_c that was not statistically significant from zero, -0.5,(-5.3 - 4.4; 95% predictive interval) Wm^{-2} and a ΔF_{net} that was nearly equal to ΔF_α, 9.3(3.7 - 14.7) Wm^{-2} (Figure 4.4A). In Scenario B, we assumed that all of the harvested pine carbon returns to the atmosphere while none of the switchgrass carbon is returned and stored. This scenario resulted in a large positive ΔF_c of 11.3(6.5 - 16.2; 95% predictive interval) Wm^{-2} and of 21.1(15.5 - 26.6) (Figure 4.4B). In scenario C, we assumed that none of the pine carbon returns to

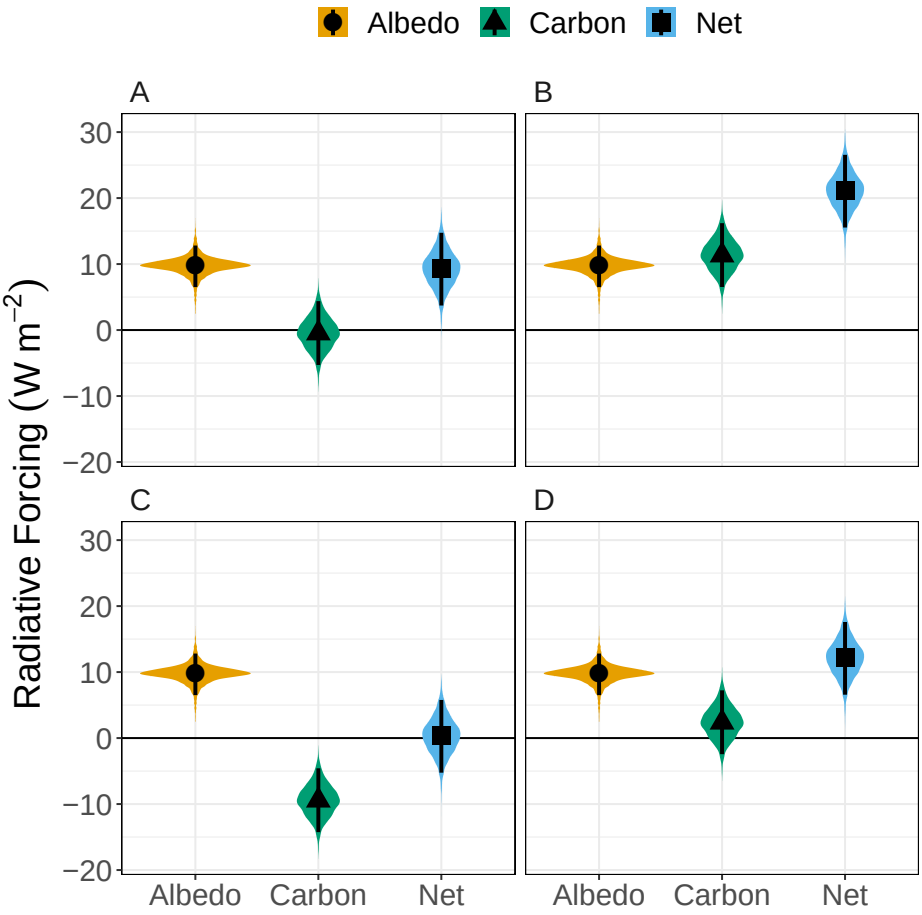

Figure 4.4: Radiative forcing(RF) from a change in land-cover over a 30 year period where; A) No harvested carbon returns to the atmosphere, B) only the pine harvest returns to the atmosphere, C) only the grass harvest returns to the atmosphere, and D) where harvested carbon from both systems enters the atmosphere. Here positive values indicate that the pine system has a warming effect on climate compared to switchgrass, and negative values mean that the pine system has a cooling effect. Points represent the mean values, lines represent the 95% prediction interval, and the violin plots show the shape of the underlying distribution.

the atmosphere, and all of the switchgrass carbon returned over the 30-year analysis period. This scenario resulted in lower ΔF_c that was equal to ΔF_α (-9.4(-14.3 - -4.6)(Figure 4.4C). As a result the ΔF_{net} near zero (0.35 Wm^{-2}; -5.2 - 5.8). Finally, in Scenario D, we assumed that all harvested carbon from both systems was returned to the atmosphere during the 30-year period. In this scenario, the literature-derived average annual yields were very similar for

the pine plantation (448 $gC\ m^{-2}\ yr^{-1}$, and switchgrass (365 $gC\ m^{-2}\ yr^{-1}$). Therefore the offsetting yields lead to very similar results to Scenario A (Figure 4.4). The average ΔF_c was 2.4(-2.4 - 7.2) Wm^{-2} and the average ΔF_{net} was 12.2(6.6 - 17.6; 95% predictive interval) Wm^{-2}. None of the four extreme scenarios resulted in a strong negative radiative forcing associated with establishing the pine plantation.

4.5 Discussion

We examined how a choice to establish a specific type of ecosystem for climate mitigation influences radiative forcing in the mid-latitudes of the eastern U.S. We found that the radiative forcing from albedo and carbon associated with a decision to establish a pine plantation rather than a switchgrass field were on the same order of magnitude and that the pine has a net positive radiative forcing when averaged over the 30-year analysis time horizon. A strength of our study was the use of site-level observations of NEP and albedo from eddy-covariance studies across eastern North America, including observations from a newly established site with co-located pine, switchgrass, and clear-cut systems. Therefore, 1) our results are not specific to a single location, 2) our results include the temporal dynamics of NEP and albedo following the establishment of the managed ecosystem, and 3) the carbon radiative forcing includes both the gains of carbon through biomass accumulation and the loss of carbon through heterotrophic respiration.

By using NEP from eddy-covariance measurements as the input for calculating the carbon radiative forcing, the radiative forcing of harvested carbon is excluded. We addressed this limitation using a sensitivity analysis and found that the radiative forcing from a change in carbon balance (ΔF_c) depended on how harvested carbon was accounted for in the calculation. Specifically, we examined the end members for the potential fate

of harvested carbon, where we assumed that all of the carbon from either loblolly pine or switchgrass was released back into the atmosphere or held in storage over the 30-year analysis horizon. While the combined 30-year mean radiative forcing was never negative (i.e., net cooling by the pine plantation) in any of the scenarios, the radiative forcing was zero (i.e., no difference between pine and switchgrass) in the scenario where switchgrass harvested carbon was returned to the atmosphere (e.g. bioenergy combustion) and pine harvested carbon was stored in wood (Figure 4.4C). Overall, this highlights that managing the fate of pine carbon that is removed can compensate but not overcome the differences in the albedo between the pine and switchgrass ecosystems. Future work can 1) refine the literature values used for harvested carbon to evaluate whether management to increase productivity and harvested carbon can alter the balance between (ΔF_c) and (ΔF_α), 2) evaluate how the offset of fossil fuel combustion through the use of harvested carbon as bioenergy influences the net radiative forcing outcome and 3) investigate how ecosystem can be managed for albedo in addition to carbon climate benefits.

Our findings are different from those reported by two other studies that use similar approaches for calculating radiative forcing of pine forests in temperate latitudes. Each of these studies found that ΔF_c exceeded ΔF_α with a combined negative radiative forcing by pine ecosystems (Betts, 2000, Kirschbaum et al., 2011). The are four primary causes of the differences. First, our study used a productive bioenergy grass ecosystem with carbon accumulation as the baseline rather than a carbon-neutral baseline as used in Kirschbaum et al. (2011) and Betts (2000). As a result the difference is carbon accumulation at the end of our analysis was only 70 $tC\ ha^{-1}$ compared to 200 and 170 $tC\ ha^{-1}$ in Kirschbaum et al. (2011) and Betts (2000). Second, our study used time-integrated NEP flux measurements from eddy-covariance sites across eastern North America to determine the (ΔF_c) rather than observations of biomass change from a single site (Kirschbaum et al., 2011) or literature values

of biomass and soil carbon (Betts, 2000). As a result of using NEP, our study includes the loss of carbon during the early stages of establishment, and those losses were greater for the pine than switchgrass ecosystems. Third, the albedo contrast between the pine and grass systems was larger in our study (8%) than Betts (2000)(5%) and Kirschbaum et al. (2011) (7%). This would result in a greater radiative forcing from albedo differences, particularly when compared to Betts (2000). Finally, each study differs in the time horizon of analysis. However, our 30-year horizon was less than the 50-year in Betts (2000) but longer than the 20-year horizon used in Kirschbaum et al. (2011), indicating that horizon is not the primary cause of the difference. Overall, the difference in carbon accumulations in both the pine and grass ecosystems is likely the most critical difference between studies.

We focus our primary conclusions on the mean 30-year average radiative forcing that emerges from albedo and NEP's temporal dynamics. The positive radiative forcing from albedo change between the pine and switchgrass systems (ΔF_α) was reduced by including the higher albedo in the early years of pine stand development. In this study, we assumed switchgrass albedo to be constant with age based on our limited observations at the Virginia site. This assumption is supported by published measurements from other studies that reported similar albedo values (Eichelmann et al., 2016b, Miller et al., 2015). Furthermore, we found that the switchgrass had similar albedo values to the bare-soil clearcut at the Virginia site, suggesting little change in albedo as bare soil transitions to vegetation during field establishment. Our study assumes that the switchgrass field had a 10-year rotation before it was replanted, resulting in three 10-year rotations to compare with a 30-year pine rotation. Ideally, we would explore the implications of longer periods between switchgrass plantings, as switchgrass can remain productive for over 20 years (Parrish and Fike, 2005). However, we could not find any published studies examining the carbon balance and albedo of switchgrass fields older than 8 years. Future work should prioritize observations of switchgrass

fields over 10 years of age.

Our analysis does not account for LCC's indirect climate effects, such as a changes in evapotranspiration and biogenic volatile organic compounds(BVOC) emissions. Previous work using climate models has found that the indirect effect of evapotranspiration, via changes in planetary albedo from altered cloudiness, can offset the direct effects of a change in albedo (Ahlswede and Thomas, 2017, Bala et al., 2007, Pongratz et al., 2011, Spracklen et al., 2008). However, at the Virginia site, we found evapotranspiration was similar between the pine and switchgrass field, so the indirect change in cloudiness and atmospheric water content may not be strongly different between the two systems (Chapter:2). However, this result may not apply to locations where decisions to establish pine or switchgrass occur, especially those with greater water stress. Therefore, additional work is necessary to examine the potential importance of evapotranspiration differences as a driver of indirect climate mitigation.

Furthermore, forests emit more BVOCs than crops and grasses, directly and indirectly influencing radiative forcing (Guenther et al., 2012, Unger, 2014). Forests in the SEUS are known for releasing large amounts of BVOCs, creating the famous Blue Ridge haze (Ferman et al., 1981). Directly, BVOCs lead to the production of organic aerosols that increases the albedo of the atmosphere. Including this direct influence of BVOCs on aerosols would potentially alter our findings by decreasing radiative forcing of the pine forest. However, few studies directly compare BVOC emissions between pine and switchgrass and some studies have found bioenergy crops to be higher emitters than other crops. Indirectly, increased BVOC emissions can increase ozone and methane in the atmosphere, both greenhouse gases, by altering the chemical reactions that governs their concentrations in the atmosphere. This would increase the radiative forcing of the pine forest. The relative roles of changes in albedo and greenhouse gases is still uncertain. In one modeling study

the reduction of BVOCs due to cropland expansion showed a net cooling effect on the same order of magnitude and in the same direction as the albedo change (Unger, 2014). However, this modeling study did not specially examine differences between switchgrass and pine ecosystems. Future work could include specific differences in BVOC emissions between pine and switchgrass ecosystems into models with interactions between vegetation, atmospheric physics, and atmospheric chemistry.

Decisions to use land-based climate solutions involve trade-offs when establishing different ecosystems for mitigation potential. Our study is a specific example that quantifies the trade-off between two managed ecosystem types in the eastern U.S. However, our conclusions likely apply to other pine plantation vs. cropland/grassland comparisons because the switchgrass albedo is typical of similar ecosystem types and our representation of uncertainty in both the NEP and albedo for the switchgrass was large enough to include variation across a wide region. Our results may not extend to a decision to establish a deciduous forest that has a higher average albedo than a pine plantation. Furthermore, forests and timber production have other indirect benefits that we did not account for here such as the substitution of timber-based building materials for emission-intensive products (O'Halloran and Bright, 2017). These indirect climate and ecosystem services may take higher precedence, given the small differences in the direct climate mitigation potential between the two ecosystems illustrated here. In conclusion, replacing switchgrass with pine plantations for the sole purpose of climate change mitigation may not be an effective strategy.This conclusion is a critical consideration if the expansion of either pine plantations or switchgrass is a component of a regional land-based climate mitigation strategy.

Chapter 5

Conclusions

Here I examined the effect that land-cover change has on local and global climate using observations of loblolly pine and switchgrass ecosystems. In chapter 2, I examined the difference in land surface temperature between loblolly pine, switchgrass, and a clearcut. I found that the presence of vegetation was the primary determinant of surface temperature. Previous works studying how land-cover change affects local climate have predominantly focused on the effects of forests with crops or grasses serving as a baseline (Burakowski et al., 2017, Juang et al., 2007, Zhang et al., 2020). Including a bare-ground ecosystem for comparison revealed that the surface temperature differences between the vegetated loblolly pine and switchgrass were small compared to differences between the vegetated systems and the bare-ground system. Additionally, other studies have found that surface-roughness changes are the primary driver of land-surface temperature differences between tall and short ecosystems (Bright et al., 2017, Burakowski et al., 2017, Lee et al., 2011, Rigden and Li, 2017). Here I found that Bowen ratio/latent heat flux differentiates between warm and cool systems. The cooling effect of latent heat flux co-varies with surface roughness (Rigden and Li, 2017). I was able to disambiguate these two processes only by comparing two short systems, one of which has periods of high latent heat flux.

In chapter 3, I examined the carbon balance and dynamics of a bioenergy switchgrass field. I found that a minimally managed, unfertilized switchgrass field in a warm-humid climate can be a source of carbon to the atmosphere. Previous studies have found switchgrass to be a sink of carbon (Chapter 3). The exact cause of this unique finding remains unclear. However, the large positive fluxes of carbon outside of the growing season at our site are not observed, or not reported, in other studies. Furthermore, the growing season at the Virginia site begins and ends earlier than other sites. Finally, the years with the most positive fluxes occurred when the harvesting of the switchgrass interrupted regrowth and when the harvested grass was left on the field for long periods of time. This suggests that

phenology and management decisions can affect the carbon balance of bioenergy crops and it is not safe to assume that all bioenergy crops are carbon sinks.

Finally, in chapter 4, I examined the radiative forcing from a change in albedo and carbon balance when converting from a switchgrass field to a pine forest. I found that the decrease of albedo and the carbon losses during pine establishment negate the carbon absorbed later in the pine life-cycle. In most cases, pine had a warming effect on global climate. Radiative forcing from this conversion only balances when all of the carbon harvested from the pine stand is prevented from entering the atmosphere. Previous work in this area has assumed that the alternative land-use to a forest is carbon neutral. Here I show that a bright, productive bioenergy crop can have greater climate benefits than a pine plantation.

Together, these findings show that there are trade-offs between local and global climate effects. During the day, the pine forest had a slightly lower average surface temperature than switchgrass, due to its persistent, year-round, latent heat flux. The high annual latent heat flux comes from the pine forest maintaining its canopy throughout the year. Due to the dark leaves, this also means that the albedo remains low throughout the year. Therefore, the slight reduction in surface temperatures comes at the cost of increased energy absorption, cooling the surface locally, but increasing radiative forcing at the top of the atmosphere. Comparing local and global climate feed-backs explicitly involves converting a change in radiative forcing at the top of the atmosphere into a temperature change at the surface. Assessing the surface temperature change due to a change in radiative forcing requires a global climate model. However, the scale of global climate models make them questionable tools for local land-use decisions. Nevertheless, the trade-offs of local and global processes should not be ignored when making a land-cover decision for climate change mitigation.

I began this work with a simple question: "Which of these two systems, switchgrass

and loblolly pine, are 'better' for climate?" The work presented here shows that the answer is complicated. However, both the global and local temperature change chapters have shown that switchgrass and pine have comparable climate benefits. Therefore the other services provided by these two ecosystems should take precedence. This balance may shift if either of the two species are replaced with less productive or longer lived species Forests are often heralded as a climate change mitigation strategy. In this project, I show that a moderately productive switchgrass field has many of the same benefits as a loblolly pine forest.

Bibliography

M. Abraha, I. Gelfand, S. K. Hamilton, C. Shao, Y.-J. Su, G. P. Robertson, and J. Chen. Ecosystem Water-Use Efficiency of Annual Corn and Perennial Grasslands: Contributions from Land-Use History and Species Composition. *Ecosystems*, 19(6):1001–1012, 2016. doi: 10.1007/s10021-016-9981-2.

M. Abraha, S. K. Hamilton, J. Chen, and G. P. Robertson. Ecosystem carbon exchange on conversion of Conservation Reserve Program grasslands to annual and perennial cropping systems. *Agricultural and Forest Meteorology*, 253-254:151–160, 2018. doi: 10.1016/j.agrformet.2018.02.016.

P. R. Adler, S. J. D. Grosso, and W. J. Parton. Life-Cycle Assessment of Net Greenhouse-Gas Flux for Bioenergy Cropping Systems. *Ecological Applications*, 17(3):675–691, 2007. doi: 10.1890/05-2018.

B. J. Ahlswede and R. Q. Thomas. Community Earth System Model Simulations Reveal the Relative Importance of Afforestation and Forest Management to Surface Temperature in Eastern North America. *Forests*, 8(12), 2017. doi: 10.3390/f8120499.

J. M. Albaugh, J.-C. Domec, C. A. Maier, E. B. Sucre, Z. H. Leggett, and J. S. King. Gas exchange and stand-level estimates of water use and gross primary productivity in an experimental pine and switchgrass intercrop forestry system on the Lower Coastal Plain of North Carolina, U.S.A. *Agricultural and Forest Meteorology*, 192-193:27–40, 2014. doi: 10.1016/j.agrformet.2014.02.013.

K. J. Anderson-Teixeira and E. H. DeLucia. The greenhouse gas value of ecosystems. *Global Change Biology*, 17(1):425–438, 2011. doi: 10.1111/j.1365-2486.2010.02220.x.

K. J. Anderson-Teixeira, A. D. Miller, J. E. Mohan, T. W. Hudiburg, B. D. Duval, and E. H. DeLucia. Altered dynamics of forest recovery under a changing climate. 19(7):2001–2021, 2013. doi: 10.1111/gcb.12194.

M. Aubinet, T. Vesala, and D. Papale, editors. *Eddy Covariance*. Springer Netherlands, Dordrecht, 2012. ISBN 978-94-007-2350-4. doi: 10.1007/978-94-007-2351-1.

D. M. Aubrecht, B. R. Helliker, M. L. Goulden, D. A. Roberts, C. J. Still, and A. D. Richardson. Continuous, long-term, high-frequency thermal imaging of vegetation: Uncertainties and recommended best practices. *Agricultural and Forest Meteorology*, 228-229:315–326, 2016. doi: 10.1016/j.agrformet.2016.07.017.

G. Bala, K. Caldeira, M. Wickett, T. J. Phillips, D. B. Lobell, C. Delire, and A. Mirin. Combined climate and carbon-cycle effects of large-scale deforestation. *Proceedings of the National Academy of Sciences*, 104(23):9911–9911, 2007. doi: 10.1073/pnas.0704096104.

D. Baldocchi. Measuring fluxes of trace gases and energy between ecosystems and the atmosphere - the state and future of the eddy covariance method. *Global Change Biology*, 20(12):3600–3609, 2014. doi: 10.1111/gcb.12649.

D. D. Baldocchi, B. B. Hincks, and T. P. Meyers. Measuring Biosphere-Atmosphere Exchanges of Biologically Related Gases with Micrometeorological Methods. *Ecology*, 69(5): 1331–1340, 1988. doi: 10.2307/1941631.

J.-F. Bastin, Y. Finegold, C. Garcia, D. Mollicone, M. Rezende, D. Routh, C. M. Zohner, and T. W. Crowther. The global tree restoration potential. *Science*, 365(6448):76–79, 2019. doi: 10.1126/science.aax0848.

R. A. Betts. Offset of the potential carbon sink from boreal forestation by decreases in surface albedo. *Nature*, 408(6809):187–190, 2000.

D. Billesbach, S. Chan, D. Cook, D. Papale, R. Bracho-Garrillo, J. Verfallie, R. Vargas, and S. Biraud. Effects of the gill-solent windmaster-pro "w-boost" firmware bug on eddy covariance fluxes and some simple recovery strategies. *Agricultural and Forest Meteorology*, 265:145–151, 2019. doi: https://doi.org/10.1016/j.agrformet.2018.11.010.

G. B. Bonan. Effects of land use on the climate of the United States. *Climatic Change*, 37 (3):449–486, 1997. doi: 10.1023/A:1005305708775.

G. B. Bonan. *Ecological Climatology*. Cambridge University Press, 2008a. ISBN 1-107-26886-9.

G. B. Bonan. Forests and Climate Change: Forcings, Feedbacks, and the Climate Benefits of Forests. *Science*, 320(5882):1444–1449, 2008b. doi: 10.1126/science.1155121.

R. Bracho, G. Starr, H. L. Gholz, T. A. Martin, W. P. Cropper, and H. W. Loescher. Controls on carbon dynamics by ecosystem structure and climate for southeastern U.S. slash pine plantations. *Ecological Monographs*, 82(1):101–128, 2012. doi: 10.1890/11-0587.1.

R. Bracho, J. G. Vogel, R. E. Will, A. Noormets, L. J. Samuelson, E. J. Jokela, C. A. Gonzalez-Benecke, S. A. Gezan, D. Markewitz, J. R. Seiler, and others. Carbon accumulation in loblolly pine plantations is increased by fertilization across a soil moisture availability gradient. *Forest ecology and management*, 424:39–52, 2018. Publisher: Elsevier.

R. M. Bright and T. L. O'Halloran. Developing a monthly radiative kernel for surface albedo change from satellite climatologies of Earth's shortwave radiation budget: CACK v1.0. *Geoscientific Model Development*, 12(9):3975–3990, 2019. doi: 10.5194/gmd-12-3975-2019.

R. M. Bright, K. Zhao, R. B. Jackson, and F. Cherubini. Quantifying surface albedo and

other direct biogeophysical climate forcings of forestry activities. *Global Change Biology*, 21(9):3246–3266, 2015. doi: 10.1111/gcb.12951.

R. M. Bright, E. Davin, T. O'Halloran, J. Pongratz, K. Zhao, and A. Cescatti. Local temperature response to land cover and management change driven by non-radiative processes. *Nature Climate Change*, 7(4):296–302, 2017. doi: 10.1038/nclimate3250.

E. Burakowski, A. Tawfik, A. Ouimette, L. Lepine, K. Novick, S. Ollinger, C. Zarzycki, and G. Bonan. The role of surface roughness, albedo, and Bowen ratio on ecosystem energy balance in the Eastern United States. *Agricultural and Forest Meteorology*, 2017. doi: 10.1016/j.agrformet.2017.11.030.

N. Cavallaro, G. Shrestha, R. Birdsey, M. A. Mayes, R. G. Najjar, S. C. Reed, P. Romero-Lankao, and Z. Zhu. Second State of the Carbon Cycle Report. Technical report, U.S. Global Change Research Program, 2018.

F. S. Chapin III, P. A. Matson, and P. Vitousek. *Principles of terrestrial ecosystem ecology*. Springer Science & Business Media, 2011.

C. Chen, L. Wang, R. B. Myneni, and D. Li. Attribution of Land-Use/Land-Cover Change Induced Surface Temperature Anomaly: How Accurate Is the First-Order Taylor Series Expansion? *Journal of Geophysical Research: Biogeosciences*, 125(9), 2020. doi: 10.1029/2020JG005787.

L. Chen and P. A. Dirmeyer. Adapting observationally based metrics of biogeophysical feedbacks from land cover/land use change to climate modeling. *Environmental Research Letters*, 11(3), 2016. doi: 10.1088/1748-9326/11/3/034002.

L. Chen, P. A. Dirmeyer, L. Chen, and P. A. Dirmeyer. Differing Responses of the Diurnal

Cycle of Land Surface and Air Temperatures to Deforestation. *Journal of Climate*, 2019. doi: 10.1175/JCLI-D-19-0002.1.

K. L. Clark, H. L. Gholz, and M. S. Castro. Carbon dynamics along a chronosequence of slash pine plantations in north Florida. *Ecological Applications*, 14(4):1154–1171, 2004. doi: 10.1890/02-5391.

R. Costanza, R. de Groot, P. Sutton, S. van der Ploeg, S. J. Anderson, I. Kubiszewski, S. Farber, and R. K. Turner. Changes in the global value of ecosystem services. *Global Environmental Change*, 26:152–158, 2014. doi: 10.1016/j.gloenvcha.2014.04.002.

N. Di Virgilio, O. Facini, A. Nocentini, M. Nardino, F. Rossi, and A. Monti. Four-year measurement of net ecosystem gas exchange of switchgrass in a Mediterranean climate after long-term arable land use. *GCB Bioenergy*, 2018. doi: 10.1111/gcbb.12523.

E. Eichelmann, C. Wagner-Riddle, J. Warland, B. Deen, and P. Voroney. Carbon dioxide exchange dynamics over a mature switchgrass stand. *GCB Bioenergy*, 8(2):428–442, 2016a. doi: 10.1111/gcbb.12259.

E. Eichelmann, C. Wagner-Riddle, J. Warland, B. Deen, and P. Voroney. Comparison of carbon budget, evapotranspiration, and albedo effect between the biofuel crops switchgrass and corn. *Agriculture, Ecosystems & Environment*, 231:271–282, 2016b. doi: 10.1016/j.agee.2016.07.007.

M. Ferman, G. Wolff, and N. Kelly. The nature and sources of haze in the shenandoah valley/blue ridge mountains area. *Journal of the Air Pollution Control Association*, 31 (10):1074–1082, 1981.

T. Foken. The Energy Balance Closure Problem: An Overview. *Ecological Applications*, 18 (6):1351–1367, 2008. Publisher: Ecological Society of America.

T. Foken, M. Göockede, M. Mauder, L. Mahrt, B. Amiro, and W. Munger. Post-field data quality control. In *Handbook of micrometeorology*, pages 181–208. Springer, 2004.

R. F. Follett, K. P. Vogel, G. E. Varvel, R. B. Mitchell, and J. Kimble. Soil Carbon Sequestration by Switchgrass and No-Till Maize Grown for Bioenergy. *BioEnergy Research*, 5 (4):866–875, 2012. doi: 10.1007/s12155-012-9198-y.

T. R. Fox, E. J. Jokela, and H. L. Allen. The development of pine plantation silviculture in the southern United States. *Journal of Forestry*, 105(7):337–347, 2007.

P. Friedlingstein, M. O'Sullivan, M. W. Jones, R. M. Andrew, J. Hauck, A. Olsen, G. P. Peters, W. Peters, J. Pongratz, S. Sitch, C. Le Quéré, J. G. Canadell, P. Ciais, R. B. Jackson, S. Alin, L. E. O. C. Aragão, A. Arneth, V. Arora, N. R. Bates, M. Becker, A. Benoit-Cattin, H. C. Bittig, L. Bopp, S. Bultan, N. Chandra, F. Chevallier, L. P. Chini, W. Evans, L. Florentie, P. M. Forster, T. Gasser, M. Gehlen, D. Gilfillan, T. Gkritzalis, L. Gregor, N. Gruber, I. Harris, K. Hartung, V. Haverd, R. A. Houghton, T. Ilyina, A. K. Jain, E. Joetzjer, K. Kadono, E. Kato, V. Kitidis, J. I. Korsbakken, P. Landschützer, N. Lefèvre, A. Lenton, S. Lienert, Z. Liu, D. Lombardozzi, G. Marland, N. Metzl, D. R. Munro, J. E. M. S. Nabel, S.-I. Nakaoka, Y. Niwa, K. O'Brien, T. Ono, P. I. Palmer, D. Pierrot, B. Poulter, L. Resplandy, E. Robertson, C. Rödenbeck, J. Schwinger, R. Séférian, I. Skjelvan, A. J. P. Smith, A. J. Sutton, T. Tanhua, P. P. Tans, H. Tian, B. Tilbrook, G. van der Werf, N. Vuichard, A. P. Walker, R. Wanninkhof, A. J. Watson, D. Willis, A. J. Wiltshire, W. Yuan, X. Yue, and S. Zaehle. Global Carbon Budget 2020. *Earth System Science Data*, 12(4):3269–3340, 2020. doi: 10.5194/essd-12-3269-2020.

A. Gelman, D. B. Rubin, and others. Inference from iterative simulation using multiple sequences. *Statistical science*, 7(4):457–472, 1992. Publisher: Institute of Mathematical Statistics.

M. Georgescu, D. B. Lobell, and C. B. Field. Direct climate effects of perennial bioenergy crops in the United States. *Proceedings of the National Academy of Sciences*, 108(11): 4307–4312, 2011. doi: 10.1073/pnas.1008779108. Publisher: National Academy of Sciences _eprint: https://www.pnas.org/content/108/11/4307.full.pdf.

A. Guenther, X. Jiang, C. L. Heald, T. Sakulyanontvittaya, T. Duhl, L. Emmons, and X. Wang. The Model of Emissions of Gases and Aerosols from Nature version 2.1 (MEGAN2. 1): an extended and updated framework for modeling biogenic emissions. *Geoscientific Model Development*, 5(6):1471–1492, 2012. Publisher: Copernicus GmbH.

J. Hansen, M. Sato, and R. Ruedy. Radiative forcing and climate response. *Journal of Geophysical Research: Atmospheres*, 102(D6):6831–6864, 1997. doi: 10.1029/96JD03436.

M. C. Hansen, P. V. Potapov, R. Moore, M. Hancher, S. A. Turubanova, A. Tyukavina, D. Thau, S. V. Stehman, S. J. Goetz, T. R. Loveland, A. Kommareddy, A. Egorov, L. Chini, C. O. Justice, and J. R. G. Townshend. High-Resolution Global Maps of 21st-Century Forest Cover Change. *Science*, 342(6160):850–853, 2013. doi: 10.1126/science.1244693.

K. S. Hemes, B. R. K. Runkle, K. A. Novick, D. D. Baldocchi, and C. B. Field. An Ecosystem-Scale Flux Measurement Strategy to Assess Natural Climate Solutions. *Environmental Science & Technology*, 55(6):3494–3504, 2021. doi: 10.1021/acs.est.0c06421.

S. Hook and G. Hulley. ECOSTRESS Land Surface Temperature and Emissivity Daily L2 Global 70 m V001 [Data set], 2019.

G. C. Hurtt, S. Frolking, M. G. Fearon, B. Moore, E. Shevliakova, S. Malyshev, S. W. Pacala, and R. A. Houghton. The underpinnings of land-use history: three centuries of global gridded land-use transitions, wood-harvest activity, and resulting secondary lands:

THE UNDERPINNINGS OF LAND-USE HISTORY. *Global Change Biology*, 12(7):1208–1229, 2006. doi: 10.1111/j.1365-2486.2006.01150.x.

IPCC. *Climate Change 2013: The Physical Science Basis. Contribution of Working Group I to the Fifth Assessment Report of the Intergovernmental Panel on Climate Change*. Cambridge University Press, Cambridge, United Kingdom and New York, NY, USA, 2013. ISBN ISBN 978-1-107-66182-0. doi: 10.1017/CBO9781107415324.

R. B. Jackson, J. T. Randerson, J. G. Canadell, R. G. Anderson, R. Avissar, D. D. Baldocchi, G. B. Bonan, K. Caldeira, N. S. Diffenbaugh, C. B. Field, B. A. Hungate, E. G. Jobbágy, L. M. Kueppers, M. D. Nosetto, and D. E. Pataki. Protecting climate with forests. *Environmental Research Letters*, 3(4):044006–6, 2008. doi: 10.1088/1748-9326/3/4/044006.

J.-Y. Juang, G. Katul, M. Siqueira, P. Stoy, and K. Novick. Separating the effects of albedo from eco-physiological changes on surface temperature along a successional chronosequence in the southeastern United States. *Geophysical Research Letters*, 34(21):L21408–5, 2007. doi: 10.1029/2007GL031296.

M. U. F. Kirschbaum, D. Whitehead, S. M. Dean, P. N. Beets, J. D. Shepherd, and A. G. E. Ausseil. Implications of albedo changes following afforestation on the benefits of forests as carbon sinks. *Biogeosciences*, 8(12):3687–3696, 2011. doi: 10.5194/bg-8-3687-2011.

N. Kljun, P. Calanca, M. W. Rotach, and H. P. Schmid. A Simple Parameterisation for Flux Footprint Predictions. *Boundary-Layer Meteorology*, 112(3):503–523, 2004. doi: 10.1023/B:BOUN.0000030653.71031.96.

X. Lee, M. L. Goulden, D. Y. Hollinger, A. Barr, T. A. Black, G. Bohrer, R. Bracho, B. Drake, A. Goldstein, L. Gu, G. Katul, T. Kolb, B. E. Law, H. Margolis, T. Meyers, R. Monson, W. Munger, R. Oren, K. T. Paw U, A. D. Richardson, H. P. Schmid, R. Staebler, S. Wofsy,

and L. Zhao. Observed increase in local cooling effect of deforestation at higher latitudes. *Nature*, 479(7373):384–387, 2011. doi: 10.1038/nature10588.

Y. Li, M. Zhao, S. Motesharrei, Q. Mu, E. Kalnay, and S. Li. Local cooling and warming effects of forests based on satellite observations. *Nature Communications*, 6(1):6603, 2015. doi: 10.1038/ncomms7603.

W. Liao, A. J. Rigden, and D. Li. Attribution of Local Temperature Response to Deforestation. *Journal of Geophysical Research: Biogeosciences*, 123(5):1572–1587, 2018. doi: 10.1029/2018jg004401.

LI-COR, Inc. *EddyPro® version 6.2.2 Help and User's Guide*. LI-COR, Inc., 2019.

S. Luyssaert, M. Jammet, P. C. Stoy, S. Estel, J. Pongratz, E. Ceschia, G. Churkina, A. Don, K. Erb, M. Ferlicoq, B. Gielen, T. Grünwald, R. A. Houghton, K. Klumpp, A. Knohl, T. Kolb, T. Kuemmerle, T. Laurila, A. Lohila, D. Loustau, M. J. McGrath, P. Meyfroidt, E. J. Moors, K. Naudts, K. Novick, J. Otto, K. Pilegaard, C. A. Pio, S. Rambal, C. Rebmann, J. Ryder, A. E. Suyker, A. Varlagin, M. Wattenbach, and A. J. Dolman. Land management and land-cover change have impacts of similar magnitude on surface temperature. *Nature Climate Change*, 4(5):389–393, 2014. doi: 10.1038/nclimate2196.

S. B. McLaughlin and L. Adams Kszos. Development of switchgrass (Panicum virgatum) as a bioenergy feedstock in the United States. *Biomass and Bioenergy*, 28(6):515–535, 2005. doi: 10.1016/j.biombioe.2004.05.006.

D. J. Mildrexler, M. Zhao, and S. W. Running. A global comparison between station air temperatures and MODIS land surface temperatures reveals the cooling role of forests. *Journal of Geophysical Research: Biogeosciences*, 116(G3), 2011. doi: 10.1029/2010JG001486. Publisher: Wiley Online Library.

J. N. Miller, A. VanLoocke, N. Gomez-Casanovas, and C. J. Bernacchi. Candidate perennial bioenergy grasses have a higher albedo than annual row crops. *GCB Bioenergy*, 8(4): 818–825, 2015. doi: 10.1111/gcbb.12291.

J. N. Miller, A. VanLoocke, N. Gomez-Casanovas, and C. J. Bernacchi. Candidate perennial bioenergy grasses have a higher albedo than annual row crops. *GCB Bioenergy*, 8(4): 818–825, 2016. doi: 10.1111/gcbb.12291.

A. Noormets. AmeriFlux US-NC2 NC_loblolly Plantation, 2016. type: dataset.

A. Noormets. AmeriFlux US-NC3 NC_clearcut#3, 2018. type: dataset.

K. A. Novick and G. G. Katul. The Duality of Reforestation Impacts on Surface and Air Temperature. *Journal of Geophysical Research: Biogeosciences*, 2020. doi: 10.1029/2019JG005543.

T. L. O'Halloran and R. M. Bright. More diverse benefits from timber versus dedicated bioenergy plantations for terrestrial carbon dioxide removal. *Environmental Research Letters*, 12(2):021001–4, 2017. doi: 10.1088/1748-9326/aa54ec.

T. L. O'Halloran, B. E. Law, M. L. Goulden, Z. Wang, J. G. Barr, C. Schaaf, M. Brown, J. D. Fuentes, M. Göckede, A. Black, and V. Engel. Radiative forcing of natural forest disturbances. *Global Change Biology*, 18(2):555–565, 2012. doi: 10.1111/j.1365-2486.2011.02577.x.

C. Oishi, K. Novick, and P. Stoy. AmeriFlux US-Dk3 Duke Forest - loblolly pine, 2016. type: dataset.

S. Pacala. Stabilization Wedges: Solving the Climate Problem for the Next 50 Years with Current Technologies. *Science*, 305(5686):968–972, 2004. doi: 10.1126/science.1100103.

D. Papale, M. Reichstein, M. Aubinet, E. Canfora, C. Bernhofer, W. Kutsch, B. Longdoz, S. Rambal, R. Valentini, T. Vesala, and D. Yakir. Towards a standardized processing of Net Ecosystem Exchange measured with eddy covariance technique: algorithms and uncertainty estimation. *Biogeosciences*, 3(4):571–583, 2006.

D. J. Parrish and J. H. Fike. The Biology and Agronomy of Switchgrass for Biofuels. *Critical Reviews in Plant Sciences*, 24(5-6):423–459, 2005. doi: 10.1080/07352680500316433.

M. Plummer. *rjags: Bayesian Graphical Models using MCMC*. 2019.

J. Pongratz, C. H. Reick, T. Raddatz, K. Caldeira, and M. Claussen. Past land use decisions have increased mitigation potential of reforestation: MITIGATION POTENTIAL OF REFORESTATION. *Geophysical Research Letters*, 38(15), 2011. doi: 10.1029/2011GL047848.

M. Reichstein, T. Kätterer, O. Andrén, P. Ciais, E.-D. Schulze, W. Cramer, D. Papale, and R. Valentini. Temperature sensitivity of decomposition in relation to soil organic matter pools: critique and outlook. *Biogeosciences*, 2(4):317–321, 2005. doi: 10.5194/bg-2-317-2005.

A. J. Rigden and D. Li. Attribution of surface temperature anomalies induced by land use and land cover changes. *Geophysical Research Letters*, 44(13):6814–6822, 2017. doi: 10.1002/2017GL073811.

M. A. Sanderson, R. L. Reed, S. B. McLaughlin, S. D. Wullschleger, B. V. Conger, D. J. Parrish, D. D. Wolf, C. Taliaferro, A. A. Hopkins, W. R. Ocumpaugh, M. A. Hussey, J. C. Read, and C. R. Tischler. Switchgrass as a sustainable bioenergy crop. *Bioresource Technology*, 56(1):83–93, 1996. doi: 10.1016/0960-8524(95)00176-X.

B. Seyednasrollah, A. Young, K. Hufkens, T. Milliman, M. Friedl, S. Frolking, A. Richardson,

M. Abraha, D. Allen, M. Apple, M. Arain, J. Baker, J. Baker, D. Baldocchi, C. Bernacchi, J. Bhattacharjee, P. Blanken, D. Bosch, R. Boughton, E. Boughton, R. Brown, D. Browning, N. Brunsell, S. Burns, M. Cavagna, H. Chu, P. Clark, B. Conrad, E. Cremonese, D. Debinski, A. Desai, R. Diaz-Delgado, L. Duchesne, A. Dunn, D. Eissenstat, T. El-Madany, D. Ellum, S. Ernest, A. Esposito, L. Fenstermaker, L. Flanagan, B. Forsythe, J. Gallagher, D. Gianelle, T. Griffis, P. Groffman, L. Gu, J. Guillemot, M. Halpin, P. Hanson, D. Hemming, A. Hove, E. Humphreys, A. Jaimes-Hernandez, A. Jaradat, J. Johnson, E. Keel, V. Kelly, J. Kirchner, P. Kirchner, M. Knapp, M. Krassovski, O. Langvall, G. Lanthier, G. Maire, E. Magliulo, T. Martin, B. McNeil, G. Meyer, M. Migliavacca, B. Mohanty, C. Moore, R. Mudd, J. Munger, Z. Murrell, Z. Nesic, H. Neufeld, T. O'Halloran, W. Oechel, A. Oishi, W. Oswald, T. Perkins, M. Reba, B. Rundquist, B. Runkle, E. Russell, E. Sadler, A. Saha, N. Saliendra, L. Schmalbeck, M. Schwartz, R. Scott, E. Smith, O. Sonnentag, P. Stoy, S. Strachan, K. Suvocarev, J. Thom, R. Thomas, A. Van den berg, R. Vargas, J. Verfaillie, C. Vogel, J. Walker, N. Webb, P. Wetzel, S. Weyers, A. Whipple, T. Whitham, G. Wohlfahrt, J. Wood, S. Wolf, J. Yang, X. Yang, G. Yenni, Y. Zhang, Q. Zhang, and D. Zona. PhenoCam Dataset v2.0: Vegetation Phenology from Digital Camera Imagery, 2000-2018. 2019. doi: 10.3334/ORNLDAAC/1674.

T. Shahzad, C. Chenu, P. Genet, S. Barot, N. Perveen, C. Mougin, and S. Fontaine. Contribution of exudates, arbuscular mycorrhizal fungi and litter depositions to the rhizosphere priming effect induced by grassland species. *Soil Biology and Biochemistry*, 80:146–155, 2015. doi: 10.1016/j.soilbio.2014.09.023.

R. H. Skinner and P. R. Adler. Carbon dioxide and water fluxes from switchgrass managed for bioenergy production. *Agriculture, Ecosystems & Environment*, 138(3-4):257–264, 2010. doi: 10.1016/j.agee.2010.05.008.

D. V. Spracklen, B. Bonn, and K. S. Carslaw. Boreal forests, aerosols and the impacts on

clouds and climate. *Philosophical Transactions of the Royal Society A: Mathematical, Physical and Engineering Sciences*, 366(1885):4613–4626, 2008.

Stacey Stewart and Robbie Berg. Hurrican Florence. Technical Report AL062018, National Hurricane Center, 2018.

J. A. Stanturf, R. C. Kellison, F. Broerman, and S. B. Jones. Productivity of southern pine plantations: where are we and how did we get here? *Journal of Forestry*, 101(3):26–31, 2003. Publisher: Oxford University Press.

C. E. Stewart, R. F. Follett, E. G. Pruessner, G. E. Varvel, K. P. Vogel, and R. B. Mitchell. N fertilizer and harvest impacts on bioenergy crop contributions to SOC. *GCB Bioenergy*, 8(6):1201–1211, 2016. doi: 10.1111/gcbb.12326.

T. Twine, W. Kustas, J. Norman, D. Cook, P. Houser, T. Meyers, J. Prueger, P. Starks, and M. Wesely. Correcting eddy-covariance flux underestimates over a grassland. *Agricultural and Forest Meteorology*, 103(3):279–300, 2000. doi: 10.1016/S0168-1923(00)00123-4.

N. Unger. Human land-use-driven reduction of forest volatiles cools global climate. *Nature Climate Change*, 4(10):907–910, 2014. doi: 10.1038/nclimate2347.

USDA-Natural Resources Conservation Service. Release Brochure for Blackwell switchgrass (Panicum virgatum). Technical report, USDA-Natural Resources Conservation Service, Manhattan PMC. Manhattan, KS 66502, 2011.

D. Vickers and L. Mahrt. Quality Control and Flux Sampling Problems for Tower and Aircraft Data. *Journal of Atmospheric and Oceanic Technology*, 14(3):512–526, 1997. doi: 10.1175/1520-0426(1997)014<0512:QCAFSP>2.0.CO;2.

P. Wagle and V. G. Kakani. Seasonal variability in net ecosystem carbon dioxide exchange

over a young Switchgrass stand. *GCB Bioenergy*, 6(4):339–350, 2014. doi: 10.1111/gcbb.12049.

D. N. Wear and J. G. Greis. The Southern Forest Futures Project: Summary Report. Article, 2012.

D. N. Wear and J. G. Greis. The Southern Forest Futures Project: technical report. Technical report, 2013.

J. Winckler, C. H. Reick, S. Luyssaert, A. Cescatti, P. C. Stoy, Q. Lejeune, T. Raddatz, A. Chlond, M. Heidkamp, and J. Pongratz. Different response of surface temperature and air temperature to deforestation in climate models. *Earth System Dynamics Discussions*, pages 1–17, 2018. doi: 10.5194/esd-2018-66.

L. L. Wright. Historical Perspective on How and Why Switchgrass was Selected as a "Model" High-Potential Energy Crop. Technical Report ORNL/TM-2007/109, 929781, 2007.

S. D. Wullschleger, E. B. Davis, M. E. Borsuk, C. A. Gunderson, and L. R. Lynd. Biomass Production in Switchgrass across the United States: Database Description and Determinants of Yield. *Agronomy Journal*, 102(4):1158–1168, 2010. doi: 10.2134/agronj2010.0087.

T. Wutzler, A. Lucas-Moffat, M. Migliavacca, J. Knauer, K. Sickel, L. Šigut, O. Menzer, and M. Reichstein. Basic and extensible post-processing of eddy covariance flux data with REddyProc. *Biogeosciences*, 15(16):5015–5030, 2018. doi: https://doi.org/10.5194/bg-15-5015-2018.

P. Yadav, P. Priyanka, D. Kumar, A. Yadav, and K. Yadav. Bioenergy Crops: Recent Advances and Future Outlook. In A. A. Rastegari, A. N. Yadav, and A. Gupta, editors, *Prospects of Renewable Bioprocessing in Future Energy Systems*, volume 10, pages 315–335.

Springer International Publishing, Cham, 2019. ISBN 978-3-030-14462-3 978-3-030-14463-0. doi: 10.1007/978-3-030-14463-0_12. Series Title: Biofuel and Biorefinery Technologies.

M. Zeri, K. Anderson-Teixeira, G. Hickman, M. Masters, E. DeLucia, and C. J. Bernacchi. Carbon exchange by establishing biofuel crops in Central Illinois. *Agriculture, Ecosystems & Environment*, 144(1):319–329, 2011. doi: 10.1016/j.agee.2011.09.006.

Q. Zhang, M. Barnes, M. Benson, E. Burakowski, A. C. Oishi, A. Ouimette, R. Sanders-DeMott, P. C. Stoy, M. Wenzel, L. Xiong, K. Yi, and K. A. Novick. Reforestation and surface cooling in temperate zones: mechanisms and implications. *Global Change Biology*, page gcb.15069, 2020. doi: 10.1111/gcb.15069.